FINAL TECHNICAL REPORT

ARPA Order Number:	3291
Program Code Number:	8F10
Name of Contractor:	Columbia University (Lamont-Doherty Geological Observatory)
Date of Contract:	01 October 1976
Contract Expiration Date:	30 September 1978
Amount of Contract:	$173,943
Contract Number:	F49620-77-C-0008 (with Amendments P00001 and P00002)
Principal Investigator:	Dr. Lynn R. Sykes (914-359-2900)
Title:	"Suture zones, seismic wave propagation, and tectonics of central Asia"

Sponsored by

Advanced Research Projects Agency (DOD)

ARPA Order No. 3291

Monitored by AFOSR Under Contract #F49620-77-C-0008

(Modified by Amendments P00001 and P00002)

ABSTRACT

The following section summarizes the projects supported by the contract.

A. An approximate method for calculating the reflection and transmission coefficients of obliquely incident Rayleigh waves across two welded quarter-spaces is outlined. The transmitted energy follows a reciprocity relation and decreases rapidly away from normal incidence; the reflected energy is small and decreases with increasing angle of incidence. This numerical method is very fast and has a low memory-storage requirement.

B. A moving-window analysis was employed to study the group velocities of fundamental mode Rayleigh and Love waves with paths traversing the Tibetan Plateau. The models derived from best-fitting these observed dispersion curves indicate that the Tibetan Plateau has an unusual crust about 70 km in thickness, with a low velocity zone at an intermediate depth within the crust.

C. Travel-time residuals determined from records of the L-DGO seismic network in the northeastern U.S. were used to map the extent of a suspected suture zone in northern New York, central Vermont, and southwestern Quebec. The results indicate that a zone of large negative residuals exists in northern New York State. Recent data also show an azimuthal dependence in the residual pattern.

D. Fault-plane solutions of moderate-sized earthquakes along the North Atlantic Ridge were determined from surface-wave amplitude spectra constrained by body-wave first motions. The strikes of the faults derived from surface wave studies agree well with the local orientation of the median valley near the epicenters. The study demonstrated that amplitudes can be used successfully to obtain reliable focal mechanism solutions for oceanic paths for periods from 25 to 80 sec.

E. A recent overview on the settings and possible causes of intraplate seismicity

reveals that the French test site in Algebra has, contrary to previous belief, not been tectonically stable since the Precambrian. The site is located in a zone that has experienced tectonic activity, including volcanism and uplift, during the past 25 million years. Seismic waves leaving this region may be more attenuated in amplitude; consequently, yield estimations for the French tests will have to take this new finding into account. The attenuation of waves from that test site may be more similar to that of waves leaving the Nevada Test Site.

The following section summarizes projects, not directly supported by the contract, but of interest to it:

A. The complicated tectonics of central Asia have been studied in several aspects. The subjects covered under this research include:

1. Detailed modelling of the Hazara region of northern Pakistan based on the mapped distribution of seismicity, composite fault-plane solutions, and geological evidences.
2. Large-scale seismotectonic trends for a portion of south-central Asia based on a compilation and critical review of the historical and modern seismicity.
3. Interpretation of the Makran region of southern Pakistan as a zone of active subduction from a detailed comparison of tectonic features in the Makran with those in a subduction environment.
4. A temporal and spatial study of seismic activity prior to the 1945 earthquake (Ms = 8) along the Makran coast of southern Pakistan.

B. Several studies concerning the seismicity and tectonics of the Aleutian Islands were carried out at L-DGO. The results of these studies may be useful in understanding other subduction zones such as the one along the Kurile Islands and Kamchatka.

1. Hypocenters, determined from data recorded by a local network in the Shumagin

Islands Alaska, define a Benioff zone that is about 10 km thick and extends to about 180 km depth. Large earthquakes appear to rupture that shallow-dipping portion of the subduction zone that occurs above 40 km depth; below that depth the Benioff zone is congruent along the entire Aleutian arc. This observation, and the low level of seismic activity at the present time in the main thrust zone compared to that in the Benioff zone below 40 km, suggest that seismic activity in the main thrust zone is dominated by great earthquakes and their aftershocks, followed by long intervals of quiescense.

2. Two high stress-drop earthquakes from the Shumagin Island, Alaska were studied in detail using data from the local short-period stations, strong-motion accelerograph (SMA), and the long-period WWSSN stations. The distribution of the mainshocks and associated aftershocks were located and mapped with high precision. The SMA data were anlyzed to give detailed source models. A tectonic interpretation for these earthquakes is given. The inferred stress drops, about 500 bars, are among the highest values known to be associated with any earthquake.
3. Seismicity in the Adak region, Alaska shows two thin zones about 25 km apart below a depth of 100 km. These zones merge at a depth of 175 km. Observed focal mechanisms showing down-dip compression in the upper zone and down-dip tension in the lower zone are predicted as the result of unbending of an elastic-plastic lithosphere.

C. A focal mechanism study and aftershocks survey were undertaken to investigate a large intraplate earthquake about 350 km southwest of Bermuda. Preliminary results are reported. That shock was situated on old oceanic crust where the attenuation of seismic waves is likely to be small. Large high frequency Pn and Sn waves were recorded in eastern North America at distances of about 15° to 20°.

D. A comparative surface-wave technique was used to precisely determine the depths of two earthquakes that occurred seaward of the Tonga trench. A focal depth of 49 km was found for a thrust-faulting earthquake, and a depth of 14 km for a normal faulting earthquake. The implied stresses are consistent with bending of an elastic plate model.

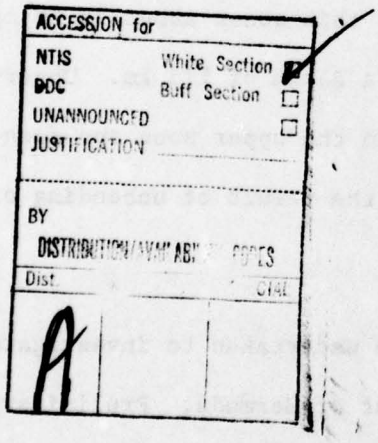

INTRODUCTION

During the past two years the Advanced Research Projects Agency (ARPA) has supported research at the Lamont-Doherty Geological Observatory of Columbia University under a contract entitled "Suture zones, seismic wave propagation, and the tectonics of central Asia". Research was undertaken to investigate the following specific problems:

1. The crustal and upper mantle structure beneath the Tibetan plateau,
2. The effect of a vertical discontinuity on the propagation of obliquely incident Rayleigh waves,
3. The characteristics and size of zones with anomalous travel-time residuals that may be caused by ancient suture zones,
4. The focal mechanisms of small-magnitude earthquakes ($m_b < 5.5$) determined by an analysis of surface waves,
5. The tectonic setting of the Algerian test site.

In addition, several other studies have been carried out at Lamont that, although supported by other contracts, are of direct interest to the subject of this contract. These studies include detailed work on the tectonics of a specific area in central Asia, regional studies of central Asian tectonics, investigations of seismicity in the Aleutians, preliminary results concerning an intraplate earthquake southwest of Bermuda, and the precise determination of depth, employing surface-wave techniques, for two earthquakes seaward of the Tonga trench.

The research program outlined above has improved our knowledge on the discrimination of nuclear explosions from natural earthquakes in several aspects. For the source region, the program has clarified our understanding on the tectonic environment in which several nuclear explosions were detonated. For the propagation path, it has attempted to quantify the effects various tectonic structures may have on the travel-time of body waves and amplitude of surface waves. The program has

Blank page

also extended the usefullness of an established discrimination method to events with small signal to noise ratio. In the following sections the methodology and results of the individual research projects are discussed.

A. Reflection and Transmission of Obliquely Incident Rayleigh Waves at a Vertical Discontinuity Between Two Welded Quarter-Spaces

An approximate method for calculating the reflection and transmission coefficients of normally incident Rayleigh waves across two welded quarter-spaces was previously outlined by Alsop, Goodman, and Gregersen (1974). Their method exploits the orthogonality property of eigenfunctions in a layered half-space to calculate the degree of matching between an eigenfunction and a wave field (Herrera, 1964). Chen and Alsop (1979) have revised two of the concepts presented in Alsop et al. (1974), then extended the revised method to allow for oblique incidence. Results for normal incidence are in agreement with previous experimental and theoretical results (McGarr and Alsop, 1969; Alsop et al., 1974). This method features two definite advantages, speed and low-memory storage requirement, over other numerical methods commonly used on surface wave transmission problems such as finite-element or finite-difference methods.

For two media with a phase velocity ratio of 1.16, they found that the transmitted energy follows a reciprocity relation; that is, if the same propagation path is followed, the energy transmitted from medium I to medium II is the same as that from medium II to medium I. Theoretically, this reciprocity relation should exist between any discrete eigenfunction on either side of a transition zone. The transmitted energy decreases from near 100% at normal incidence to 50% at about 40° (Figure 1a). The reflected energy is less than 1% and decreases with increasing angle of incidence (Figure 1b). Extending their calculations to refracted angles beyond the critical angles of S to P and S to S conversions, they found that the transmitted energy continues to follow the reciprocity relation and decreases further.

Reflected energy remains below 1% but fluctuates irregularly; no total internal reflection is observed.

Since Chen and Alsop did not take boundary conditions on the free surface into account, they believe that the calculated energy for reflection/transmission will be reduced by diffractive effects, and their results probably represent an overestimate for the reflected and transmitted energy. They are presently working on the calculation of Rayleigh waves across a vertical discontinuity in two layered quarter-spaces, and will compare the theoretical results with observations from an ocean-bottom seismograph and an adjacent land station.

B. Crustal and Upper Mantle Structure of the Tibetan Plateau

A knowledge of the velocity and attenuation structure beneath the Tibetan Plateau is important for the discrimination of explosions detonated in the Sinkiang Province, China and eastern Kazakh, U.S.S.R. To determine crustal models for the Tibetan plateau Chun and Yoshii (1977) and Chun (personal communication, 1977) determined the group velocities of fundamental mode Rayleigh and Love waves in the period range 5-100 sec. A moving window analysis was employed.

The models derived from these observed dispersion curves (Figure 2) indicate that the Tibetan plateau has an unusual crust about 70 km in thickness. Crustal velocities are generally low (Figure 3). From the abundant volcanoes in the region, the low velocities are inferred to be caused by high temperatures at crustal depth. A low velocity zone at an intermediate depth within the crust appears to be well constrained by the observed dispersion data.

C. Travel-Time Study of Anomalous Crust and Upper Mantle Structure in the Northeastern United States

Slabs of mantle-like material imbricated in the upper crust during the suturing

of two continental masses can result in an anomalous zone of high velocity material. Seismic waves that pass through such zones will be affected in travel-time, and possibly in waveform and amplitude. The delineation of their effects are important for the accurate locating of nuclear explosions and the computation of their yields.

Travel-time residuals determined from records of the L-DGO seismic network in the northeastern U.S. were used to map the extent of a suspected suture zone in northern New York, central Vermont and southwestern Quebec. The travel-time residuals are computed for impulsive P-wave arrivals from both teleseismic earthquakes and explosions. Preliminary residuals are computed for each station by using the Jeffreys-Bullen tables. The average of these preliminary station residuals is then subtracted from each individual residual to produce the final residual. In this way errors caused by source, path or other effects common to all stations, hopefully are removed.

To date eighteen events have been examined. The results tend to confirm the observations of Fletcher et al. (1978) that a zone of large negative residuals exists in northern New York State and along the St. Lawrence River (Figure 4). The recent data indicate that the residual pattern is azimuthally dependent. The residuals range from -1.8 to -0.5 sec for events to the north and west, but are negligible for other directions. Data previously suggestive of a similar zone of large negative residuals in the greater New York City region are conflicting in the light of recent data.

The zone of negative residuals in northern New York State, central Vermont, and southern Quebec may result from mantle material that was thrust into the crust in this region during the suturing of the rest of North America and New England in Ordovician times. Outcrops of mafic material in this region support such an interpretation. Further research is still needed to determine if anomalous amplitudes and waveforms can be documented and to apply this method to other regions where suture zones are suspected (such as the numerous suture zones of Asia).

D. Surface Wave Studies of Small-Magnitude Earthquakes from the Mid-Atlantic Ridge

For earthquakes from the mid-ocean ridges, a combination of conditions at the source and receiver often makes focal mechanism studies using first motion difficult. At the source, the moderate size of the mid-ocean ridge earthquakes and the strong attenuation of the low-velocity zone there combine to result in small and emergent first motions (Solomon, 1973). In addition, most long-period observational stations are located at teleseismic distances from mid-ocean ridges, so that most stations fall into a dilational quadrant for normal-faulting events. Thus, the orientations of the nodal planes are often difficult to resolve.

Recent developments in normal mode theory (Saito, 1967) and signal processing (e.g. Landisman et al., 1969) have made the analysis of surface waves, which usually have the largest amplitude on a long-period seismogram, into a more common method in the study of fault-plane solutions (Forsyth, 1975). There is, however, a major drawback in the surface wave approach in that it requires a large amoun of signal-processing. Mid-ocean earthquakes, by nature of their peculiar tectonic setting, require less data-processing when using the surface wave approach to obtain fault-plane solutions. It is well known that mid-ocean ridge earthquakes have either normal- or strike-slip-faulting mechanisms (Sykes, 1967), and they are usually shallow (Weidner and Aki, 1975). Normal mode theory for Rayleigh waves predicts that for shallow events, normal-faulting will generate a two-lobed radiation pattern with amplitude nodes along the fault strike, but strike-slip-faulting will generate a four-lobed radiation pattern with amplitude nodes along the strikes of both conjugate nodal planes. Therefore, Rayleigh wave radiation patterns from mid-ocean earthquakes will be informative to their fault-type and approximate orientation of fault strike. Ho and Sykes have used this property to study the focal mechanisms of some moderate-sized ($4.6 \leq Ms \leq 5.6$) earthquakes in the North Atlantic Ocean (Table 1, Figure 5A).

Long-period, vertical component seismograms from the WWSSN were selected from circum-Atlantic stations. The seismograms were then digitized and interpolated at 1-s intervals. A moving-window analysis (Landismen et al., 1969) with a window length 7 times the period was performed on each record to obtain the amplitude spectra. They then corrected the amplitude spectra for instrument response, geometrical spreading and attenuation using a general Q model (Tsai and Aki, 1969). The spectral densities at any specific period were then plotted as a function of epicentral azimuths (Figure 5B-E). The amplitude nodes in the Rayleigh wave radiation pattern, together with constraints from body wave first motions, allow them to resolve the fault-type and the strike of the faults to $\pm$ 15°. The strikes of the faults derived from surface wave studies agree well with the orientation of either the mediam valley or fracture zones near the epicenters.

E. Attenuation at the Algerian Test Site

There have been several studies in which the amplitudes of the seismic waves emitted from explosions at the French test site in Algeria were measured to estimate the seismic yields from these explosions. In these studies the tectonics of the Algerian site were assumed to be typical of a continental shield. In an extensive review on intraplate seismicity, Sykes (1978) points out that the region of the French test site has, contrary to previous belief, not been tectonically stable since the Precambrian. The region was reactivated during the separation of Africa from the Americas, and has experienced volcanism during the past 25 million years. Such regions of reactivation tend to follow old zones of weakness along the edges of cratons. The French test site is, therefore, located in a zone that has experienced tectonic activity, including volcanism and uplift, during the past 25 million years. Seismic waves leaving this region may be severely attenuated in amplitude. This situation is quite similar to the Nevada Test Site, a region that has also

experienced late Tertiary and Cenozoic volcanism. Hence, amplitude-yield curves for the Algerian test-site probably cannot be directly applied to estimating yield for sites that have been tectonically stable for hundreds of millions of years.

II. RELATED STUDIES

The following section summarizes research that, although not supported directly by the contract, is of interest to the subject of the contract.

A. Tectonics of Central Asia

The tectonics of central Asia are complicated. In contrast to the relatively simple structures observed at subduction zones, those structures that were produced in response to the collision between continental India and Eurasia are not as well understood. In this section we describe several projects carried out at L-DGO that concern central Asian tectonics.

1. Seismic activity recorded by a network of telemetered stations in northern Pakistan has recently revealed a detailed picture on the structures and processes currently affecting the Hazara region. By unraveling the complicated situation that exists there, it may now be possible to understand the tectonics of other regions in central Asia that are characterized by a similar environment. Such regions may include the eastern termination of the Himalayan structures where several anomalous earthquakes have occurred.

The Hazara region of northern Pakistan is an arcuate belt of foreland folds and thrusts that extends from the western Himalayan syntaxis to the Sulaiman Range (Figure 6A, B). A model based on the mapped distribution of microseismicity, composite fault-plane solutions, and geological evidence was constructed to explain the recent tectonic processes of this region (Seeber and Jacob, 1977; Armbruster et al., 1978; Seeber and Armbruster, 1979). The *Indus-Kohistan Seismic Zone* and the Hazara Lower Seismic Zone are major zones of displacement within the basement (Figure 7); the former is the more active of the two. These zones appear to be extensions of the Himalayas beyond the western Himalayan syntaxis. The Hazara Lower Seismic Zone seems to merge upward and to the south with a shallow-dipping surface of décollement that decouples the basement from the overlying sediments and metasediments (which have a thickness of between 10 to 30 km) (Figure 8). The décollement surface is probably lubricated by Infracambrian salt.

2. On a braoder scale, the historical and modern seismicity (Figures 9 and 10) for a portion of south central Asia has been compiled and critically reviewed to reveal the large-scale seismotectonic trends (Quittmeyer and Jacob, 1979; Quittmeyer et al., 1979). It is difficult to associate individual earthquakes with specific mapped faults for the following reasons: (1) areas are mapped only in a reconnaissance fashion, (2) the locations of the earthquakes are of limited precision, and (3) the density of faults is sometimes high. In some cases, however, seismicity can be associated with faults or zones of faulting. This seismicity includes large earthquakes and their associated aftershocks, and well defined lineations of earthquakes with small to moderate magnitudes.

3. The Makran region of southern Pakistan has been the subject of two moderately detailed studies. Jacob and Quittmeyer (1979) showed that volcanic, geologic and seismic evidences are consistent with the interpretation of the Makran region as a zone of active subduction. If rigid plate assumptions are made and the poles and rotation rates of McKenzie (1972), McKenzie and Slater (1971) and Minster et al. (1974) are used, it is found that oceanic portions of the Arabian plate subduct northwards towards Eurasia at a rate of about 5 cm/yr. Most of the tectonic features associated with the arc-trench system are extreme. For instance: (1) the arc-trench gap measures 500 $\pm$ 100 km in width, (2) the Benioff zone is only weakly developed to a depth of 80 km, (3) the volcanic chain shows wide spacing (> 100 km) between major centers of activity, and (4) a large portion of the accretionary prism is subaerially exposed (see Figures 11 and 12). Two focal mechanisms in the deepest part of the documented Benioff zone exhibit down-dip tension. One great earthquake (M_s = 8) in 1945 ruptured a section of the plate boundary.

4. Seismic activity prior to the 1945 earthquake along the Makran coast of southern Pakistan was consistent with patterns identified by Kelleher and Savino (1975) and Mogi (1969) before other large earthquakes (Quittmeyer, 1979). Although

the data are sparce, the seismic activity inland (probably within the subducted slab) for earthquakes with magnitude 6 to 7 appears to be higher for the period 20 to 10 years before the great coastal earthquake than in any 10 year period after it. In addition, activity occurred along the coast only in the vicinity of the impending 1945 epicenter (Figure 13A-D). The region that was seismically active, both before and after the 1945 shock, is now relatively quiet.

B. Tectonics of the Aleutian Seismic Zone

A number of studies concerning the Aleutian seismic zone are currently being pursued at L-DGO. These studies increase our knowledge of the configuration of a typical subduction zone and some of the interesting earthquakes that have occurred in it. The results of these studies may be applicable to understanding other subduction zones such as the Kuriles and Kamchatka.

1. A seismic network has been operated in the Shumagin Islands and adjacent Alaska Peninsula, Alaska since July 1973. Hypocentral cross-sections based on the first four years' data from this network show a well-defined Benioff zone that is about 10 km thick and extends to about 180 km depth (Davies and House, 1978). Focal mechanism and strong-motion accelerograph data for an m_b = 6.0 earthquake at 40 km depth indicate a slip plane subparallel to the Benioff zone. This event is interpreted as being directly caused by the underthrusting of the Pacific lithosphere beneath the Shumagin Islands. Comparison of the Shumagin hypocentral cross-section with cross-sections from other regions of the Aleutian arc show that at depths greater than 40 km (1) the Benioff zones are nearly congruent and (2) their positions relative to the volcano line are nearly the same along the entire length of the arc. This comparison also reveals that the eastward widening of the volcano-trench separation occurs predominantly in the shallowly dipping extension of the Benioff zone from its position at 40 km depth to where it outcrops near the trench; this extension is herein termed the main thrust zone. Rupture zones of the 1964, 1965, and possibly, the 1938 great earthquakes along the Aleutian arc are confined to the main thrust zone. This observation and the very low level of seismic activity at the present time in the main thrust zone compared to that in the Benioff zone below 40 km depth suggest that seismic activity in the main thrust zone is dominated by great earthquakes and their aftershocks, followed by long intervals of quiescence. The Benioff zone below 40 km depth shows more continual seismic

activity. For the Aleutian arc there exists a weak correlation between the width of the main thrust zone and the rupture length and magnitude (Mw) of great earthquakes. 2. Earthquakes with high stress-drop generate an unusually large amount of high-frequency seismic waves. They also have a large m_b compared to M_s. Since these seismic characteristics are similar to those of nuclear explosions, close examination of such high stress-drop earthquakes may further our understanding on the limitation of this discrimination method.

Two moderate-size earthquakes (m_b = 5.8, 6.0), with high estimated stress drops, occurred on April 6, 1974, beneath the Shumagin Islands (Alaska) within a local network of short-period seismograph stations. These earthquakes triggered a strong-motion accelerograph (SMA) at Sand Point (SDP) (Figure 14).

P arrivals for the two mainshocks and 29 aftershocks were picked with a precision of 0.05 sec on seismograms recorded by 5 local stations. The locations of these earthquakes are presented in a cross-sectional view in Figure 15. The hypocenters define a plane dipping at about 30° to the NW (Figure 15B). Figure 15A is a view normal to the local Wadati-Benioff zone. This figure shows that the aftershock zones for the two mainshocks, although close together, are relatively distinct. Linear dimension (diameter) of the aftershock zone is about 3-4 km for the m_b = 5.8 event, and about 4-5 km for the m_b = 6.0 event.

Long period data from the WWSSN were used to determine the focal mechanism of the 0356, m_b = 6.0 earthquake (Figure16). P-wave first motions alone are insufficient to constrain either nodal plane. The addition of S-wave polarizations refines the mechanism determination considerably and places limits on its uncertainty. The tectonic setting and the trend of the aftershocks favor the choice of the NW dipping nodal plane as the fault plane. Focal parameters for the fault plane are: strike = 254° $\pm$ 15°, dip = 30° $\pm$ 5°, and rake of slip vector = 90° $\pm$ 15°.

Analysis of the SMA records was carried out using a circular-fault version of a quasi-dynamic model (Boatwright, 1978b, 1979). A description of this technique,

summarized from Boatwright (1978b, 1978), follows:

The S-wave signals were digitized, corrected for instrument-response, and rotated to S_V and S_H components. Since the S_H amplitudes were less than 10% of those for S_V, the analysis was restricted to the S_V component only.

Accelerograms, corrected for the effect of free surface, are shown in Figures 17 and 18, as well as respective velocity and V^2 traces. Note the remarkable similarity of the V^2 plots in pulse shapes and amplitudes for the two events. The events probably share a similar rupture geometry and velocity.

Detailed source models, derived from the circular version of the quasi-dynamic model, have an "elliptical" or self-similar slip distribution and causal healing. The displacement spectra for these two events fall off more steeply than ω^{-2}. The sharp falloff indicates a gradual stopping of the rupture. This feature was also incorporated into the model. Final model parameters are listed in Table 2. The high stress-drops for these two earthquakes may indicate either a regional stress build-up prior to a large earthquake or the release of a localized high strength region (asperity) that was unbroken by the most recent (1938) major earthquake. The calculated stresses are among the highest computed for any seismic gap in the world. Archambeau (preprint) has also obtained a high stress-drop estimate for several recent earthquakes in the Shumagin region.

3. Seismicity located using the Adak seismograph network shows the Benioff zone below a depth of 100 km consists of two thin zones of earthquakes about 25 km apart that merge at a depth of 175 km. Focal mechanisms in the upper zone are consistently down-dip compression, while those of the lower zone are down-dip tension. An elastic plastic model of the lithosphere predicts that these two zones reflect the stresses in the elastic core of the lithosphere due to unbending (Engdahl and Scholz, 1977).

C. North-Atlantic Intraplate Earthquake of 24 March 1978: Preliminary Results

On March 24, 1978, an intraplate earthquake of magnitude 6 occurred about 350 km southwest of Bermuda, in seafloor of Mesozoic age (near magnetic anomaly M4; $\sim$ 117 my B.P.). Teleseismic records of this shock were analyzed to obtain a fault-plane solution. An aftershock survey was conducted from June 17-24, 1978, to study the settings and possible causes of this intraplate earthquake. Since several test sites also have intraplate environments (e.g. - NTS, Algeria, India and several in the U.S.S.R.), it is important to understand the causes and characteristics of intraplate earthquakes so that we may discriminate them from nuclear tests in intraplate environments.

The aftershock survey, conducted in cooperation with Woods Hole Oceanographic Institution, deployed sonobuoy and ocean bottom hydrophone (OBH) arrays. Conflicting locations reported for the mainshock resulted in the misalignment of the array away from the center of aftershock activity. Nevertheless, numerous events were recorded. Preliminary results place the cluster of aftershock activity at 29°50'N, 67°20'W.

The main shock was of thrust type. Data at hand are, however, insufficient to constrain the orientation of the nodal planes. The investigation of this earthquake is continuing.

This series of shocks has an excellent set of high frequency observations at intermediate distances (about 15° to 25°) which are of great importance to the understanding of the detection-discrimination levels that a network in the U.S.S.R. could provide.

D. Detailed Study of Two Earthquakes Seaward of the Tonga Trench: Implications for Mechanical Behavior of the Oceanic Lithosphere

Two nearby earthquakes seaward of the Tonga trench, one normal-faulting and one thrust-faulting, were studied in detail using comparative, surface wave techniques. The techniques require the epicenters of two earthquakes to be close to each other so that the effects of propagation and station response for common stations would be the same for both events. By looking only at relative amplitudes of the two events at each station, much of the scatter can be removed. In addition, since the propagation paths are similar, the relative phases of the Rayleigh waves at each station can be compared. The observed amplitudes, corrected for the effects of propagation and station response, and observed focal phases were fitted with theoretical patterns to obtain the best-fitting focal mechanism solutions. The focal depth for the thrust-faulting event was found to be 49 km below sea-level, consistent with the focal depth estimated from pP-P delay time. The normal-faulting event had a depth of 14 km.

These are the first precise depth determinations for earthquakes which are associated with the bending of oceanic lithosphere before subduction. The pattern of horizontal deviatoric tension near the surface and compression within the interior of the lithosphere is consistent with the stresses predicted by an elastic plate model, although the depth of the thrust event suggests that either the elastic layer begins near the base of the crust or that the rheological model should be modified to include a plastic layer of finite strength (Chen and Forsyth, 1978).

The ability to determine precise depth estimates for seismic events is one important aspect of a nuclear discrimination program.

TABLE 1

SUMMARY OF EARTHQUAKE DATA

Event	Latitude (°N)	Longitude (°W)	Date	Origin Time (hr min sec)	Magnitude (m_b)	Type of Faulting
1	31.03	41.49	11 Nov 65	15 24 40.8	6.0	Normal
2	32.26	41.03	06 Aug 62	01 35 27.7	---	?
3	33.79	38.64	28 Mar 76	20 19 45.8	5.5	?
4	35.20	35.37	17 Apr 74	00 32 21.4	5.0	Strike-Slip

TABLE 2

Derived Source Parameters

0153-event

Radius - $a = 1.2$ km

Moment - $M_o = 3.5 \pm .8 \times 10^{24}$ dyne·cm

Stress drop - $\Delta\sigma = 890$ bars Range 600-1100 bars

Effective Stress - $\tau_e = 1040 \pm 350$ bars

Radiated Energy - $E_s = 8.7 \pm 3.0 \times 10^{20}$ dyne·cm

Apparent Stress - $\tau_a = 160 \pm 60$ bars

0356-event

Radius - $a = 1.65$ km

Moment - $M_o = 6.7 \pm 1.5 \times 10^{24}$ dyne·cm

Stress Drop - $\Delta\sigma = 650$ bars Range 350-800 bars

Effective Stress - $\tau_e = 780 \pm 250$ bars

Radiated Energy - $E_s = 12.4 \pm 4.0 \times 10^{20}$ dyne·cm

Apparent Stress - $\tau_a = 120 \pm 50$ bars

FIGURE CAPTIONS

Figure 1. a. Percentage of energy transmitted as a function of angle in polystyrene.

b. Percentage of energy reflected as a function of incident angle.

Figure 2. Group velocities for Rayleigh and Love waves across the Tibetan Plateau.

a. The earthquakes (filled circles) and WWSSN stations (open circles) used in the study. The Tibetan Plateau is strippled; the Indo-Gungetic basin is hatched.

b. Group velocities for the paths in (a). The smallest dot represents one data point; the largest dot represents three or more data points superimposed.

c. Averaged group velocities for Rayleigh and Love waves. The bars indicate twice the RMS value of the residuals. Previously published Rayleigh-wave data by Gupta and Narain (1967), Santo and Sato (1966) and Chen and Molnar (1975) are also shown.

Figure 3. a. Acceptable shear wave models (TP-2, TP-3, and TP-4) for the Tibetan Plateau. Note the low-velocity zone at depths of about 25 to 40 km. Also shown for comparison is the Canadian Shield model CANSD (Brune and Dorman, 1963).

b. Vertical cross section along 85°E as shown in Figure 3a by the solid line X-X'. TP-4 is from this study. Other seismic models compiled are: (1) Bhattacharya (1971), (2) Gangetic model of Chun and Yoshii (1977), (3) Chen and Molnar (1975) and (4) Gupta and Narain (1967). Depth to the "Moho" is from a Chinese tectonic map (Tectonic Map Compiling Group, 1974 - solid line), and deduced from gravity data (Kono, 1974 - dashed line).

Figure 4. See Figure.

Figure 5. a. Approximate location of earthquakes studied (filled circle) and the WWSSN stations used in surface wave study of shocks from mid-Atlantic Ridge.

b. - e. The amplitude spectral densities plotted as a function of azimuth for events 1 to 4, respectively. The spectral densities are given at the following periods: event 1, 35.7 sec, event 2, 35.7 sec, event 3, 35.7 sec, event 4, 65.0 sec. Event 1 (Figure 5B) shows a two-lobed radiation pattern typical of shallow normal-faulting earthquakes. Event 4E shows a four-lobed radiation pattern, signifying strike-slip faulting. Radiation patterns for events 2 and 3 are ambiguous, and cannot resolve the fault type.

Figure 6. a. Regional setting of the Hazara region in northern Pakistan. Areas other than Quaternary basins are dotted.

b. Seismic stations (triangles) comprising the Tarbela Dam (TD) and Chashma Power Plant (near CR) networks. Structural features are shown for reference and are the same as shown in Figure 7.

Figure 7. Six months of epicentral data from the Tarbela and Chashma networks. Only earthquakes of magnitude 0.5 or greater are shown. The seismicity plotted is representative of the longer term activity as recorded by the networks. The concentration of activity in the upper right that has a northwest-southeast trend is the Indus Kohistan Seismic Zone (IKSZ). The Hazara Lower Seismic Zone parallels the IKSZ about 80 km to the southwest. Geologic features are shown in thinner lines; faults identified from seismic data are shown in thicker lines. Line X-X' represents the projection line of the cross-section shown in Figure 8.

Figure 8. A vertical projection of the seismicity along a 20 km wide northeast-trending strip across the Tarbela network. All good hypocenter locations between August 1973 and August 1976 are included. Solid triangles are seismic stations. The average topographic relief is indicated. Composite fault-plane solutions are projected on hemispheres convex to the southeast (towards the viewer). Solution 12 is for earthquakes west of the HLSZ west of the Indus River (not shown in the section). Faults are drawn as suggested by hypocenter alignments; directions of motion are from the composite solutions. The thrusting motion indicated for the low-angle fault is conjectural.

Figure 9. Map of maximum documented intensity (Modified Mercalli Scale) at any given location. Data for the time period ∿ 25 A.D. to 1972 are shown; however, mapped portions of the U.S.S.R. and China are not considered, and data from Iran are insufficient for quantitative description. Isoseismal lines (dotted where inferred) are plotted for some of the larger events. The year of occurrence for each such large event is indicated. The intensity value associated with a given isoseismal line is indicated in the box near each date. The first value given is for the innermost isoseismal line, etc. A few locations for which a documented intensity is known are not plotted so that isoseismal lines will be more clearly visible. The open triangles represent some major cities.

Figure 10. Epicentral map of modern seismicity for the region studied. The filled squares are proportional to magnitude and represent earthquakes recorded at teleseismic distances from January, 1914 through April, 1975. The symbol labelled UD in the magnitude scale denotes events with undetermined magnitude. Events from 1914 to 1964 are relocated. No distinction is made between surface-wave and body-wave magnitudes in this figure. Four large earthquakes ($M_s > 7$) that occurred from 1905 to 1914 are represented by open circles.

Figure 11. Tectonic sketch map of the Makran region and surrounding vicinities. The abyssal part of the oceanic portion of the Arabian plate (in the Gulf of Oman), that is, the area with water depths larger than 3000 m, is shown in dark diagonal hatching. Note the distribution of ophiolite belts and "colored mélanges" on land (solid dark areas). In some cases, they may indicate the approximate locations of probable former continent/ocean boundaries in the late Mesozoic/early Cenozoic. Also note that the pattern of present drainage divides (light ring patterns) mimics approximately the plate boundaries and the triple junction, probably as they may have existed some 30 (or more) m.y. ago. Deep sediment-filled interior basins, probably with recent histories of subsidence, are shown in light shading. Of these, the Jaz-Murian and the Hamun-i-Mashkel depression are interpreted by Farhoudi and Karig (1977) as forearc basins; they lie seaward of the volcanic arc. Note the linear arrangement of the volcanic edifices in the approximately 450 km long and less than 100 km wide volcanic arc. The three major Quaternary volcanic centers - the Koh-i-Sultan (elevation 2,510 m), Taftan (4,100 m), and Bazman (3,490 m) - are spaced more than 100 km apart, but connected by numerous small volcanic plugs and edifices. The volcanic arc strikes approximately ENE and cuts diagonally across numerous tectonic surface

features. The carbonatite volcano Koh-i-Khan Nasin in the Helmand Basin of Afghanistan (upper center) is probably not part of the Baluchistan volcanic arc which produces mostly rocks of andesitic, calc-alkaline composition.

Figure 12. Cross section XX' (along 60°E from 24° to 30°N) through the western Makran region showing the earthquake hypocenters and inferred dipping Benioff zone (bottom), and topography and some surface tectonic features (top) along the same profile. Bottom: Circles represent events up to 200 km to the east of the section line, triangles up to 200 km to the west. Filled symbols represent events for which the depth is constrained by at least one depth phase; open symbols represent events for which the depth is determined by minimizing the residuals of first P arrivals only. Average depths determined independently by these two methods usually differ by no more than 10 km in cases when both are availsble in this region. The events labelled A and B are those for which fault plane solutions were determined. The arrows at these two hypocenters show the plunges of the T axes for these two events, taking into account the 2X vertical exaggeration. The shaded band is the inferred upper boundary of the descending oceanic lithosphere belonging to the Arabian plate. Top: Major tectonic features and subdivisions of the trench-volcano gap in the western Makran. Note the coincidence in the portion of trench-slope break at the southern boundary of the subsiding forearc basin (Jaz Murian depression) with the sudden deepening of the Benioff zone from crustal (< 40 km) to sub-crustal depths. The development of these forearc basins may be closely related to a sudden steepening in the dip of the descending oceanic lithosphere beneath it (Jacob et al., 1977). Note the different vertical exaggerations in the top and bottom of the Figure.

Figure 13. Seismicity of the Makran region during different time periods. The magnitude-quality scale (note: there is no differentiation among A, B, and C quality events) is shown in part A; the distance scale is shown in part B. Events for which a magnitude could not be determined are plotted as if they had a magnitude of < 4.9. The epicenter of the great earthquake in 1945 is represented by a cross enclosed in a circle in parts A, C, and D. The major centers of Quaternary volcanism are indicated by filled circles surrounded by radiating line segments.

A. Seismic activity before the 1945 earthquake. Activity is located north and northwest of the 1945 rupture zone and in the vicinity of the 1945 epicenter. The region west of this activity is relatively quiet. The two earthquakes in the southeast corner of the map are associated with the Murray ridge.

B. The great 1945 earthquake and its long-term aftershock activity. The largest symbol (filled circle) represents the epicenter of the 1945 event. The long-term aftershock activity suggests a rupture length of 100 to 200 km to the east of the main shock epicenter. The region northwest of the rupture zone is now relatively quiet; the region west of the rupture zone remains quiet.

C. Seismicity after the decline in long-term aftershock activity. During this period of time the entire Makran region exhibits a low level of activity.

D. Recent seismicity of the Makran region. An increased number of earthquakes are detected because of the establishment of the WWSSN. Most of these events would not have been detected during an earlier time period. Activity along the coast, west of the 1945 epicenter produces a "donut" pattern. One earthquake of moderate magnitude, located to the northwest of the donut pattern, may be analogous to the activity that preceded the 1945 event.

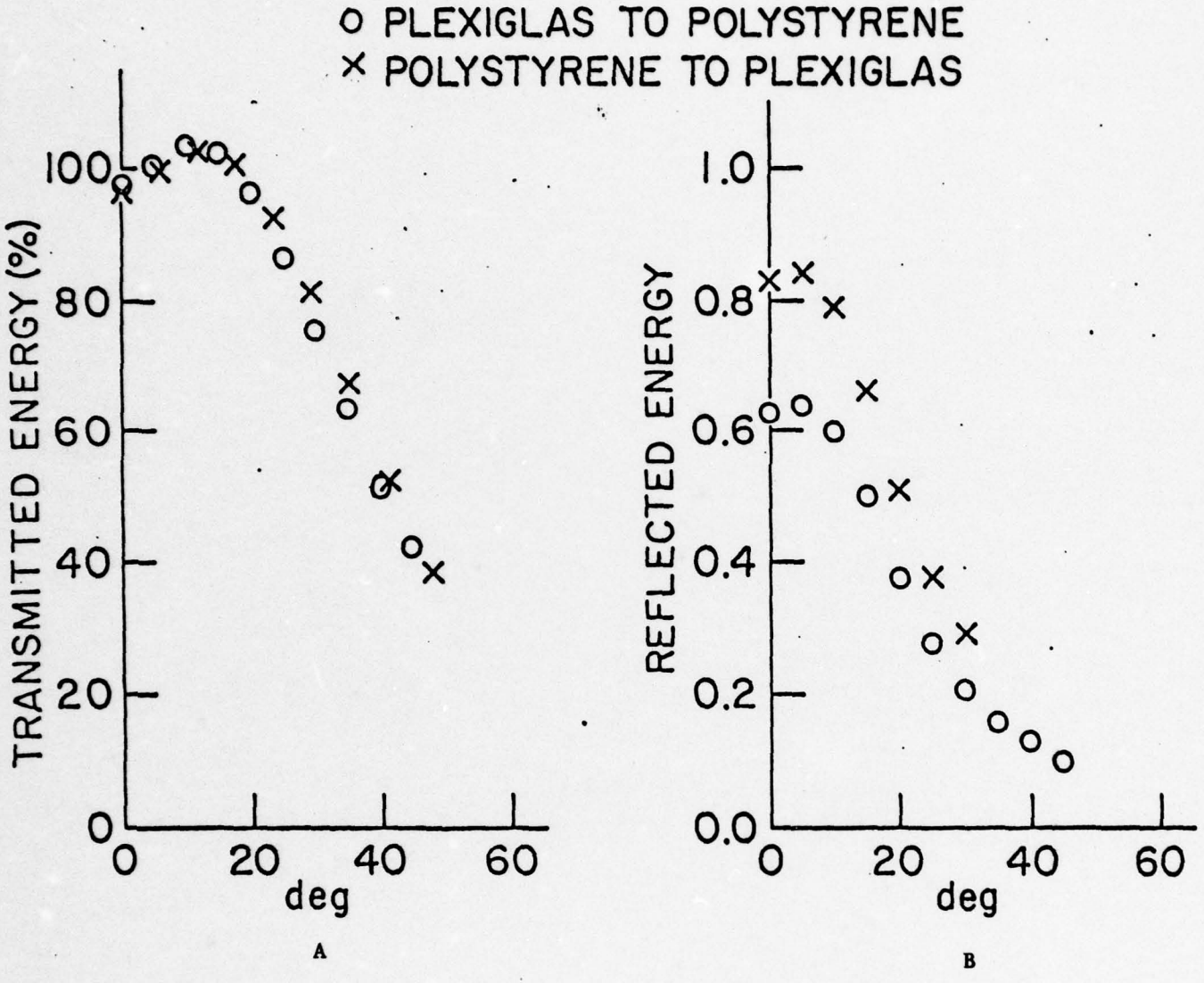
o PLEXIGLAS TO POLYSTYRENE
× POLYSTYRENE TO PLEXIGLAS
TRANSMITTED ENERGY (%)
100
80
60
40
20
0
0
20
40
60
deg
A
REFLECTED ENERGY
1.0
0.8
0.6
0.4
0.2
0.0
0
20
40
60
deg
B

FIGURE 1

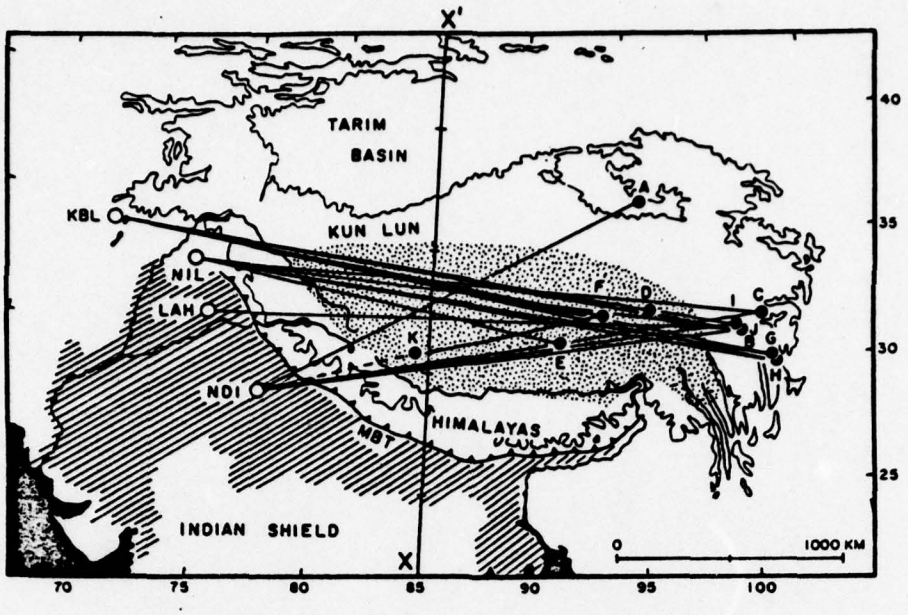
X'
TARIM
BASIN
KUN LUN
KBL
NIL
LAH
NDI
MBT
HIMALAYAS
INDIAN SHIELD
X
0
1000 KM
70
75
80
85
90
95
100
40
35
30
25

A

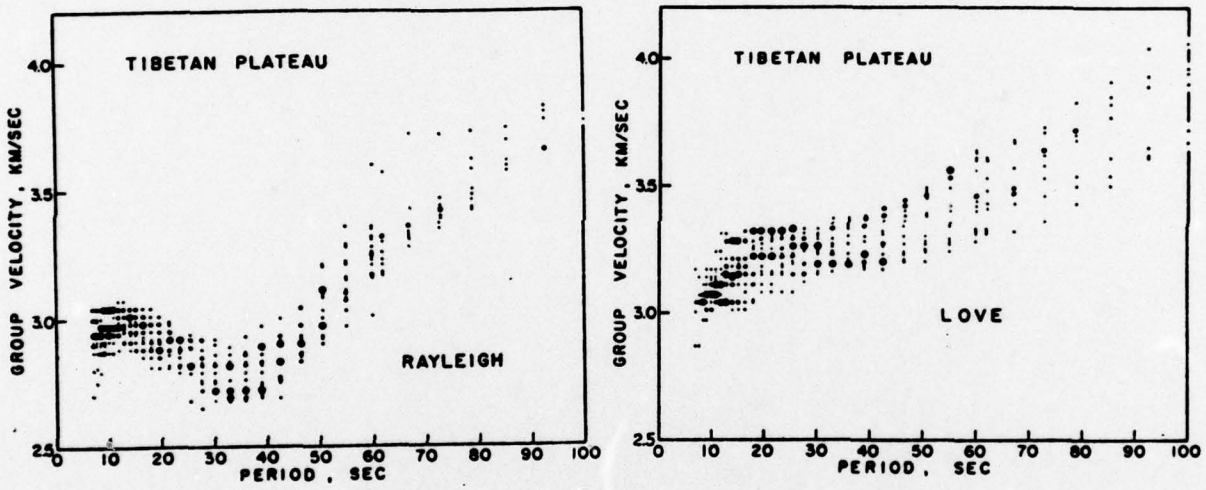
TIBETAN PLATEAU
RAYLEIGH
GROUP VELOCITY, KM/SEC
PERIOD, SEC
TIBETAN PLATEAU
LOVE
GROUP VELOCITY, KM/SEC
PERIOD, SEC

B

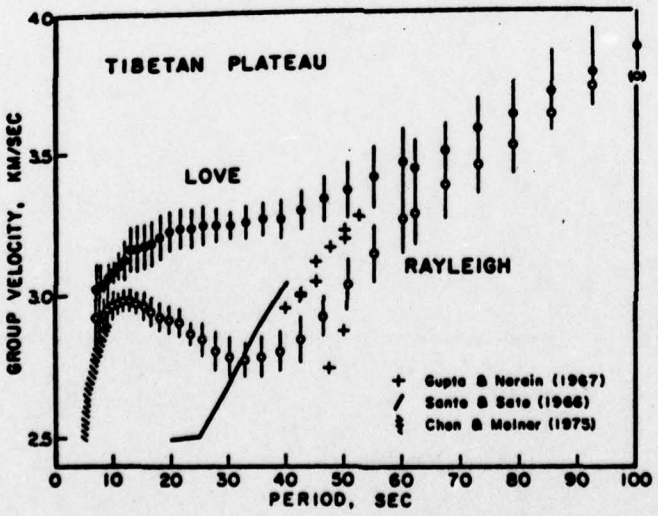
TIBETAN PLATEAU
LOVE
RAYLEIGH
Gupta & Narain (1967)
Santo & Sato (1966)
Chen & Molnar (1975)
GROUP VELOCITY, KM/SEC
PERIOD, SEC

C

FIGURE 2

A

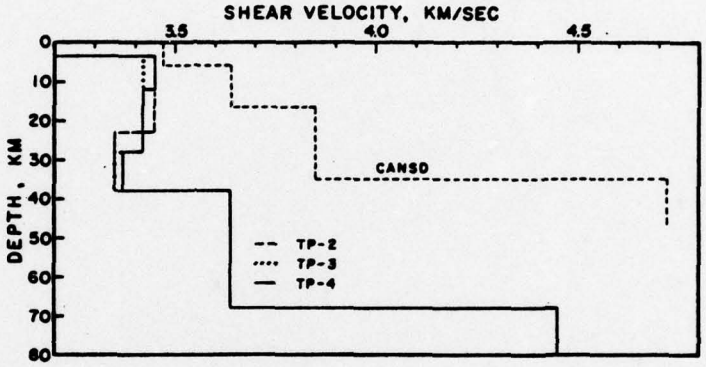
SHEAR VELOCITY, KM/SEC
3.5
4.0
4.5
DEPTH, KM
0
10
20
30
40
50
60
70
80
CANSD
TP-2
TP-3
TP-4

B

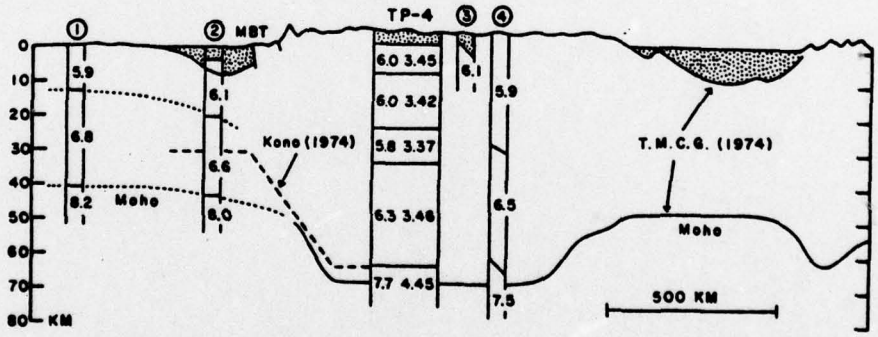
①
②
MBT
TP-4
③
④
5.9
6.8
8.2
Moho
6.1
6.6
8.0
Kono (1974)
6.0 3.45
6.0 3.42
5.8 3.37
6.3 3.46
7.7 4.45
6.1
5.9
6.5
7.5
T.M.C.G. (1974)
Moho
500 KM
KM

FIGURE 3

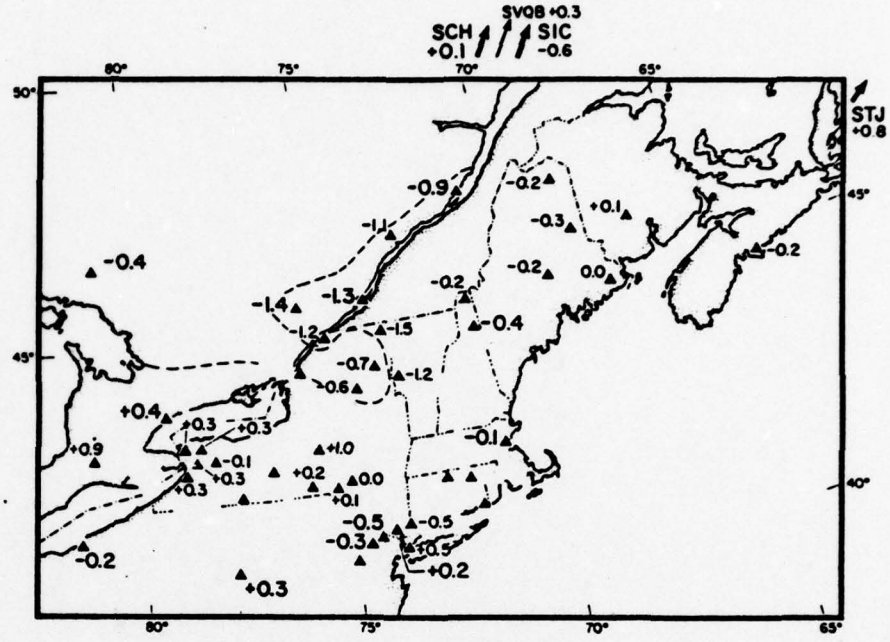

Figure 4a. Normalized travel-time residuals at individual stations in northeastern United States and adjacent parts of Canada for Cannikin, Milrow, and Longshot explosions in Aleutians. Individual readings and standard deviations are listed in Table 1 (see footnote 1). Dashed line = boundary between rocks of Precambrian age to north and younger rocks to south. Note zone centered in northern New York and southern Quebec where all residuals are unusually negative by −0.6 to −1.5 s. Larger numbers indicate that residual was determined from two or more explosions with standard deviation less than 0.35 s. Smaller symbols denote readings from either single explosions or averages with larger standard deviations.

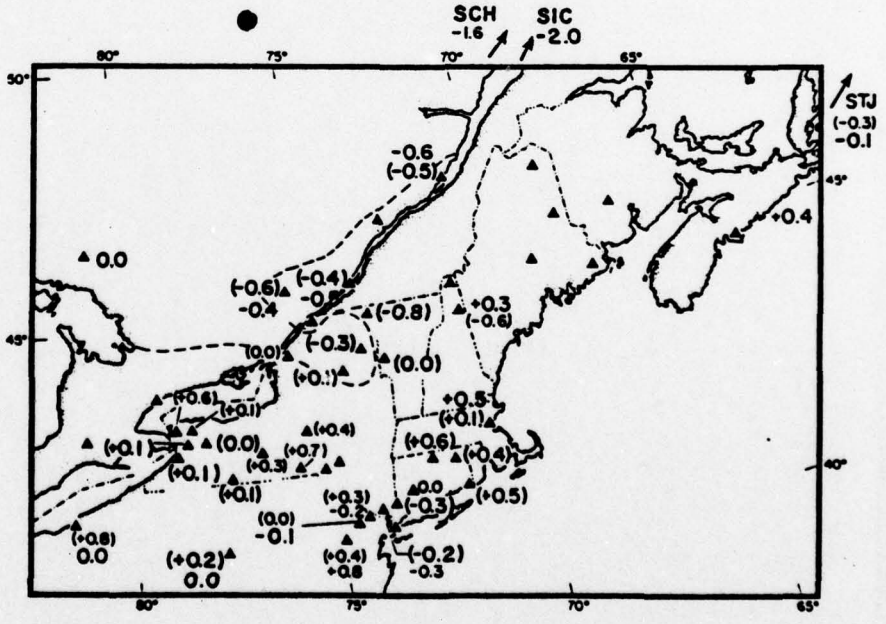

Figure 4b. Normalized travel-time residuals for explosions at Novaya Zemlya USSR (in parentheses) and Nevada Test Site. Size of symbols same as Figure 4a Data in Table 1 (see footnote 1).

A

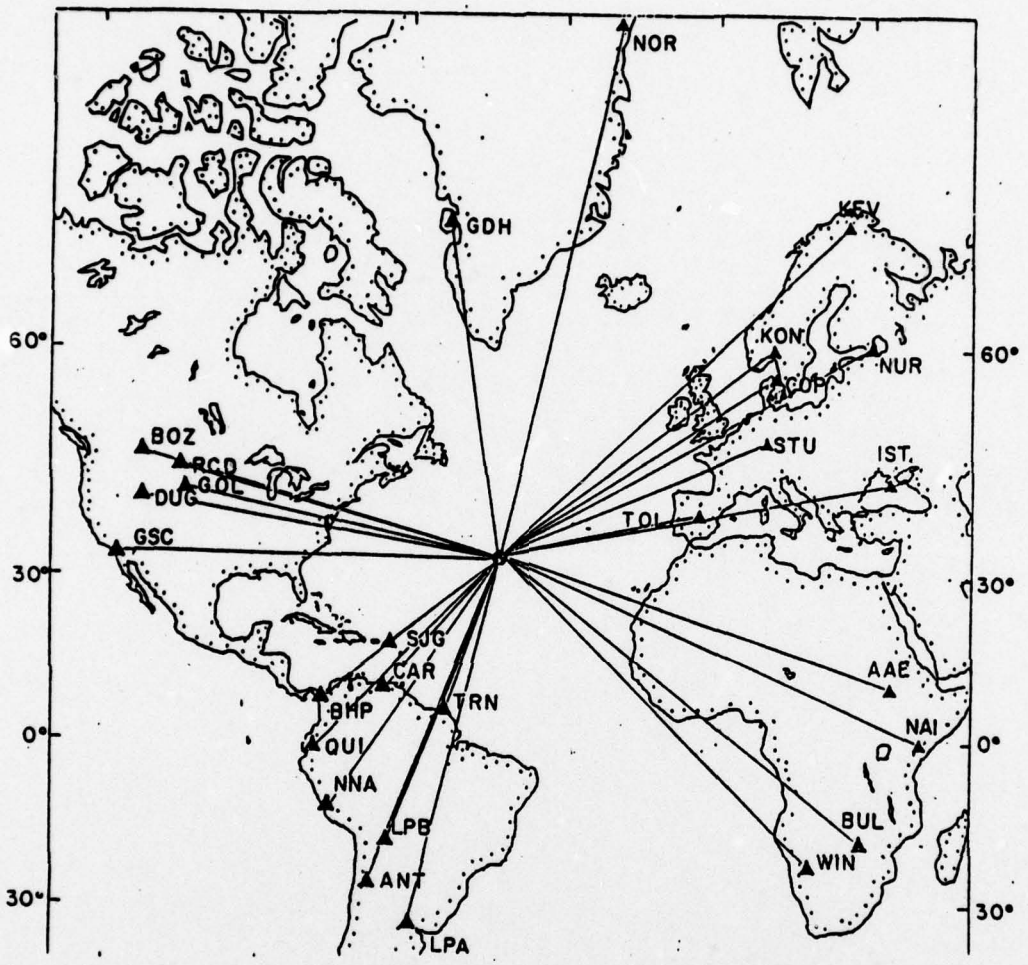
NOR
GDH
KEV
KON
NUR
COP
STU
IST
TOI
BOZ
RCD
GOL
DUG
GSC
SJG
CAR
BHP
TRN
QUI
NNA
LPB
ANT
LPA
AAE
NAI
BUL
WIN
60°
30°
0°
30°
60°
30°

FIGURE 5

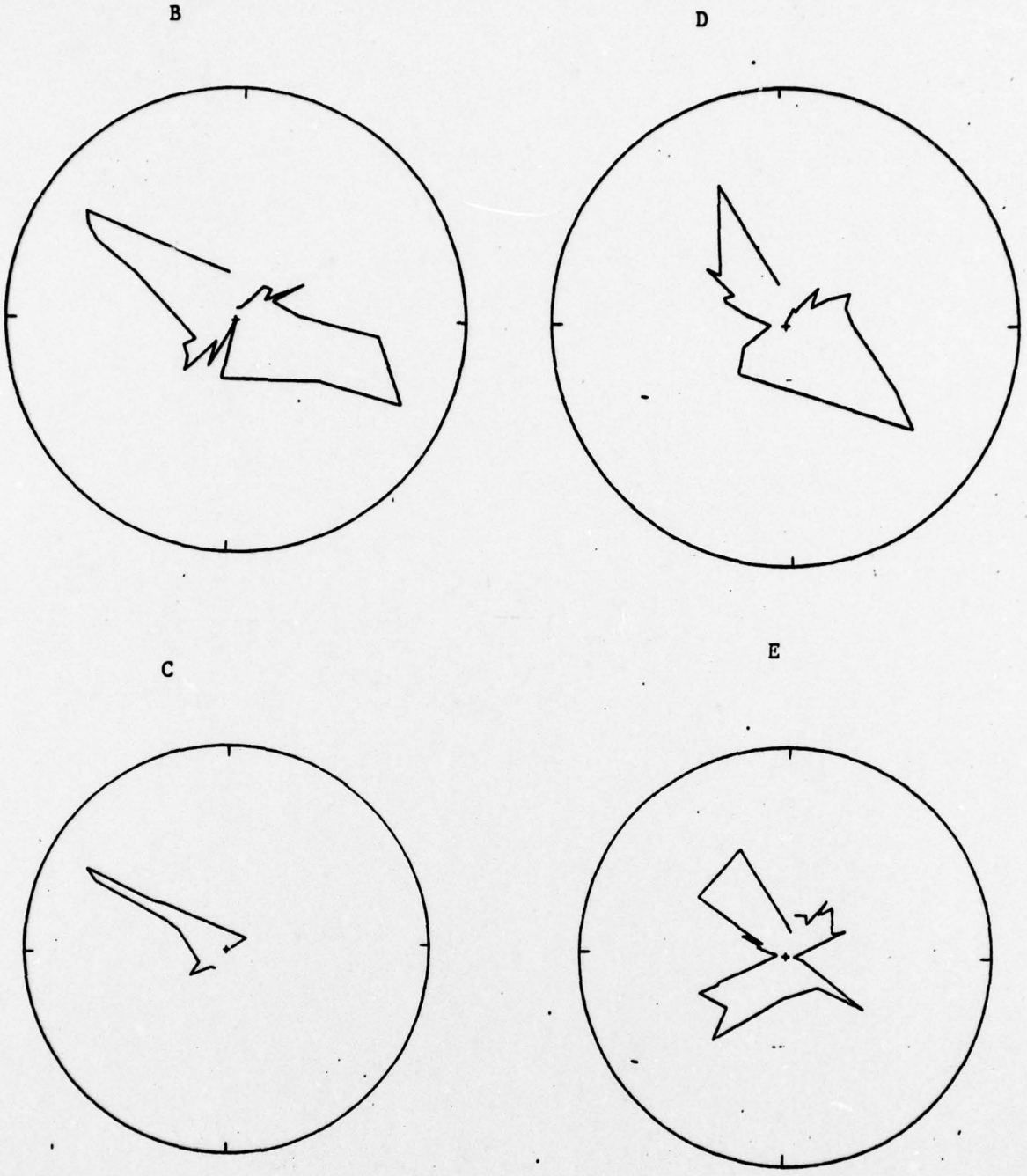

FIGURE 5

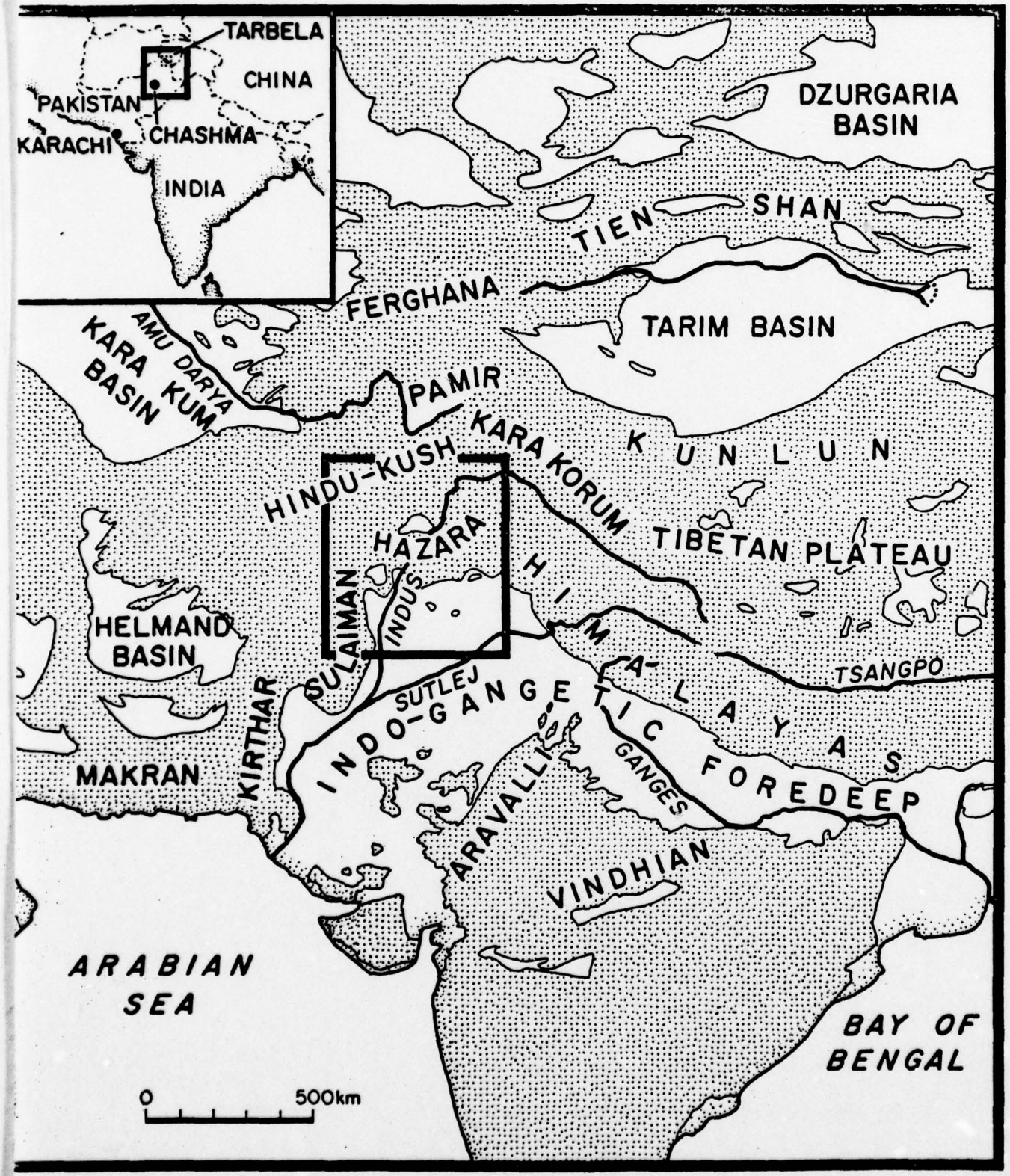
TARBELA
CHINA
PAKISTAN
CHASHMA
KARACHI
INDIA
DZURGARIA BASIN
TIEN SHAN
FERGHANA
TARIM BASIN
AMU DARYA
KARA KUM BASIN
PAMIR
KARA KORUM
K U N L U N
HINDU-KUSH
HAZARA
TIBETAN PLATEAU
SULAIMAN
INDUS
H I M A L A Y A S
HELMAND BASIN
TSANGPO
SUTLEJ
INDO-GANGETIC FOREDEEP
KIRTHAR
MAKRAN
ARAVALLI
GANGES
VINDHIAN
ARABIAN SEA
BAY OF BENGAL
0
500km

FIGURE 6A

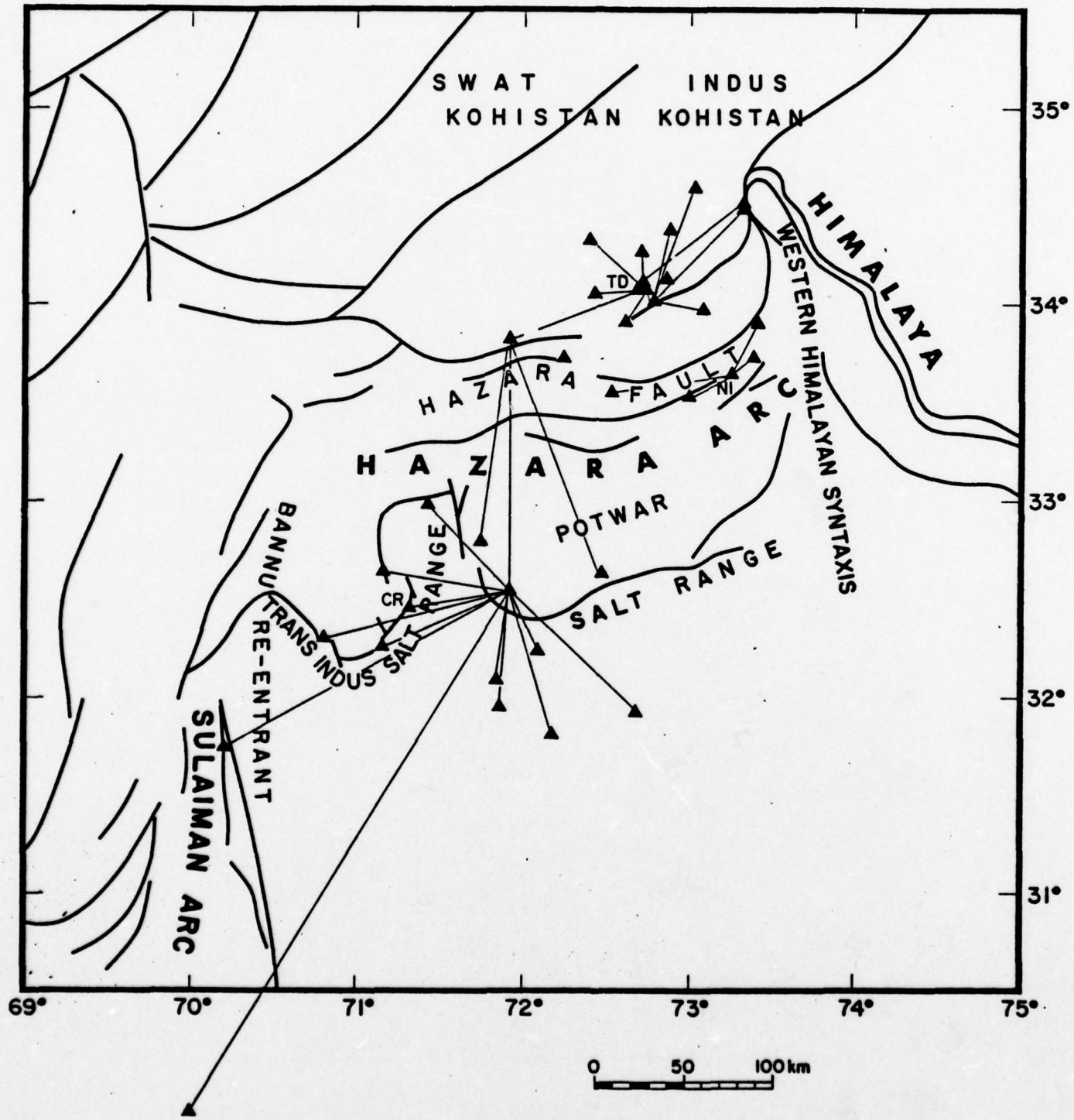
SWAT KOHISTAN
INDUS KOHISTAN
HIMALAYA
WESTERN HIMALAYAN SYNTAXIS
TD
HAZARA FAULT
NI
HAZARA ARC
POTWAR
SALT RANGE
CR
BANNU TRANS INDUS SALT RANGE
RE-ENTRANT
SULAIMAN ARC
35°
34°
33°
32°
31°
69°
70°
71°
72°
73°
74°
75°
0 50 100 km

FIGURE 6B

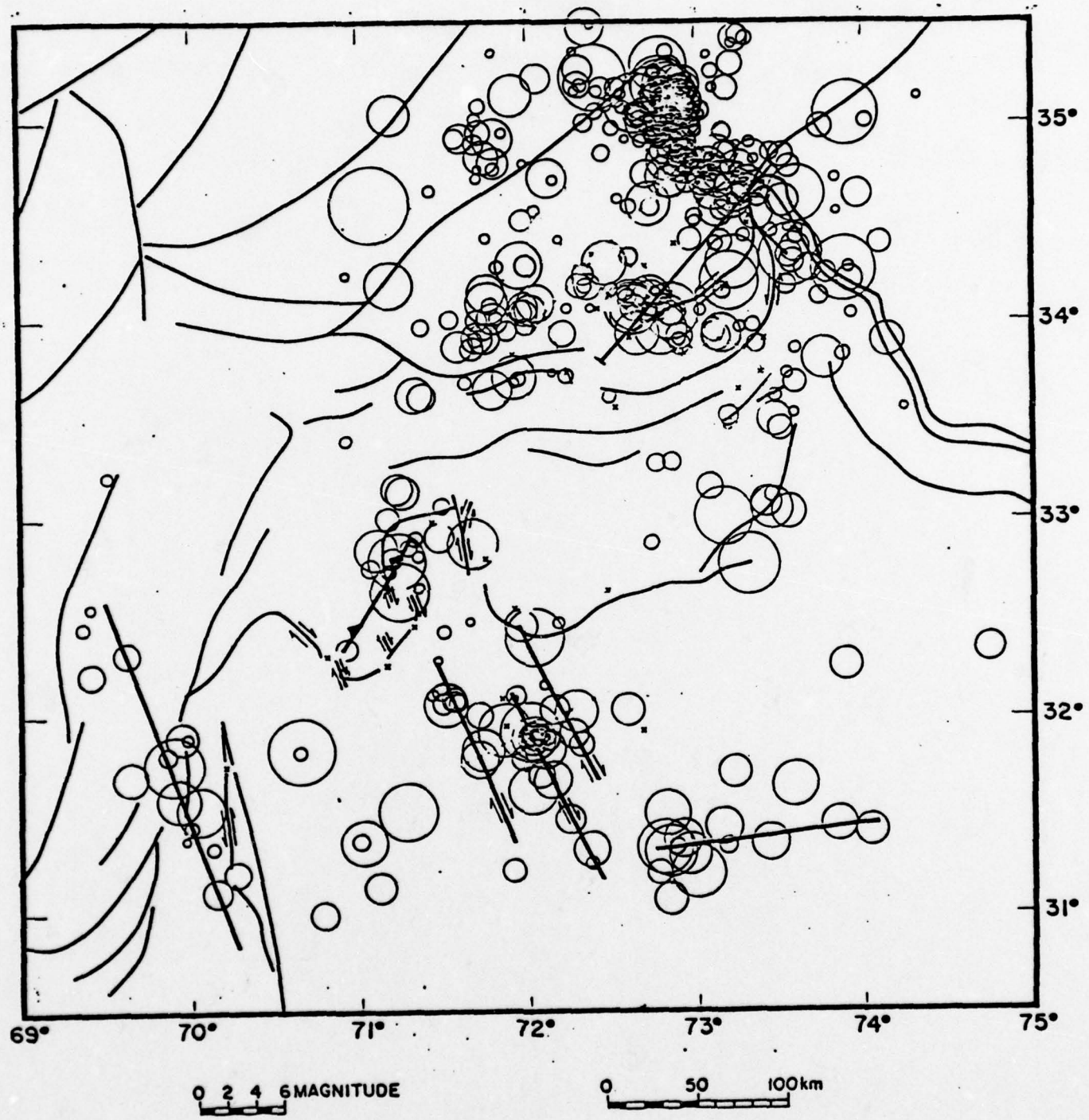

FIGURE 7

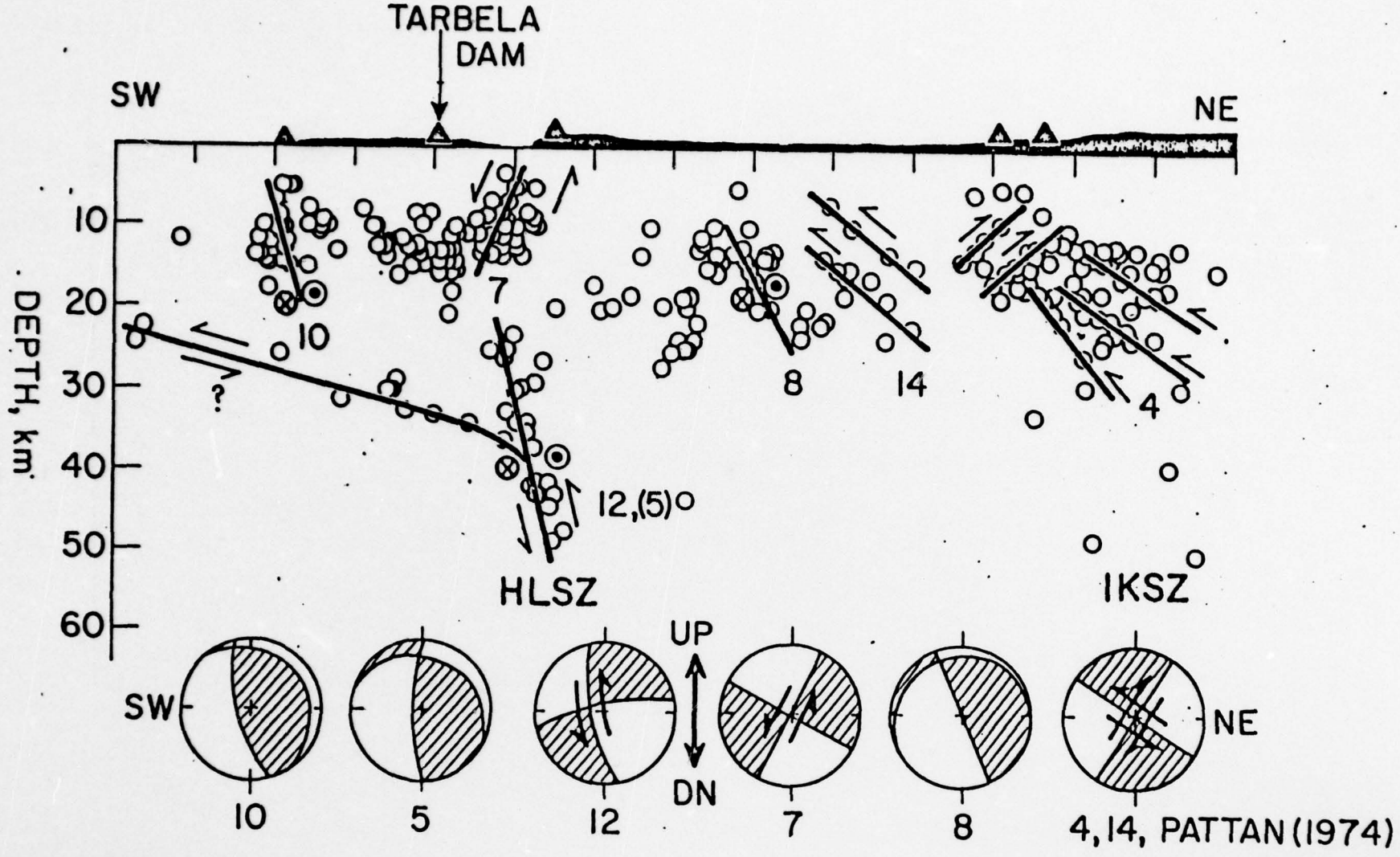
TARBELA
DAM
SW
NE
DEPTH, km.
10
20
30
40
50
60
10
7
10
?
8
14
4
12,(5)
HLSZ
IKSZ
UP
DN
SW
NE
10
5
12
7
8
4,14, PATTAN (1974)

FIGURE 8

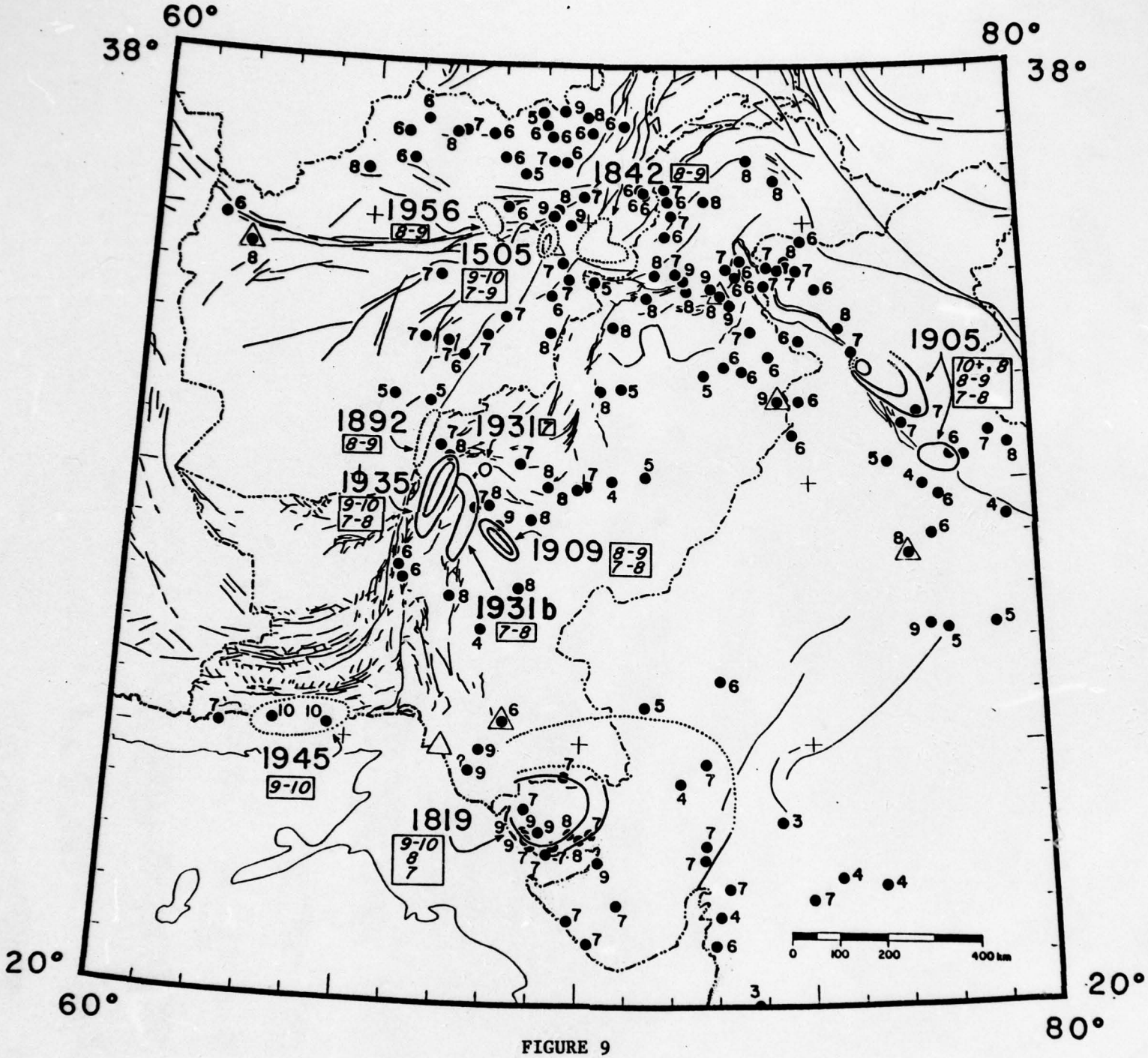
60°
38°
80°
38°
1842
8-9
+1956
8-9
1505
9-10
7-9
1905
10+, 8
8-9
7-8
1892
8-9
1931
1935
9-10
7-8
1909
8-9
7-8
1931b
7-8
1945
9-10
1819
9-10
8
7
0 100 200 400 km
20°
60°
80°
20°

FIGURE 9

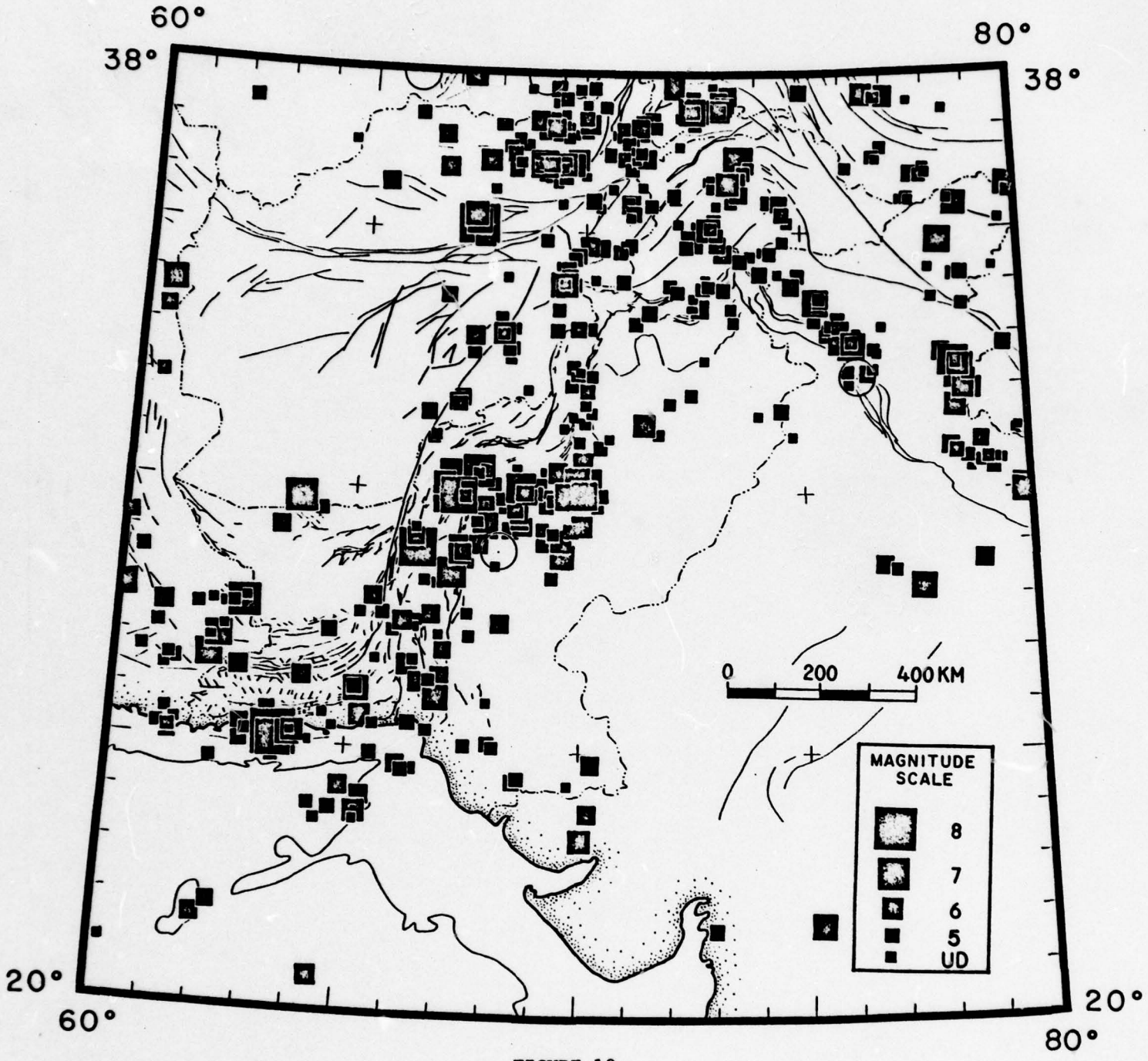

FIGURE 10

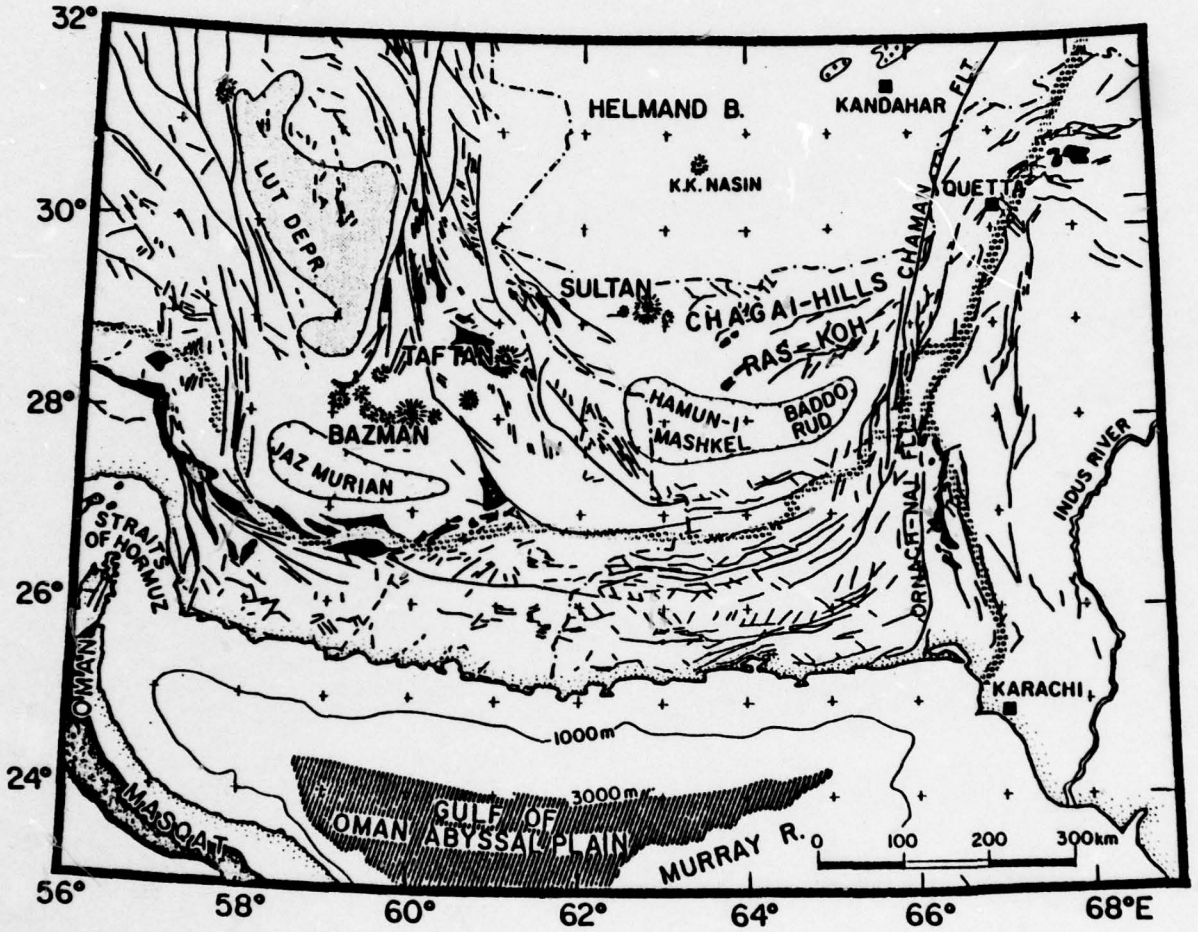
32°
30°
28°
26°
24°
56°
58°
60°
62°
64°
66°
68°E
HELMAND B.
KANDAHAR
K.K. NASIN
QUETTA
LUT DEPR.
SULTAN
CHAGAI-HILLS
CHAMAN FLT
RAS-KOH
TAFTAN
HAMUN-I-MASHKEL
BADDO RUD
BAZMAN
JAZ MURIAN
STRAITS OF HORMUZ
OMAN
ORNACH-NAL FLT
INDUS RIVER
KARACHI
1000m
3000m
GULF OF OMAN ABYSSAL PLAIN
MASQAT
MURRAY R.
0 100 200 300km

FIGURE 11

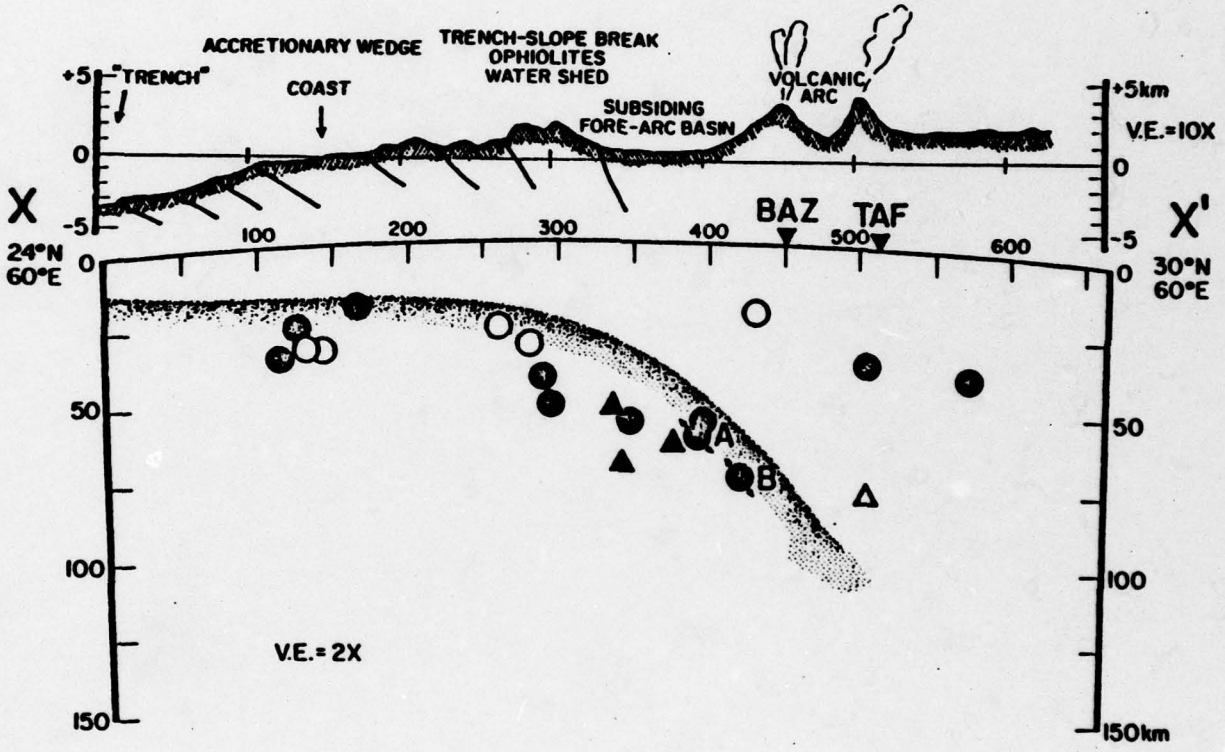
ACCRETIONARY WEDGE
TRENCH-SLOPE BREAK
OPHIOLITES
WATER SHED
"TRENCH"
COAST
SUBSIDING
FORE-ARC BASIN
VOLCANIC
ARC
+5km
V.E.=10X
+5
0
-5
X
X'
BAZ
TAF
100
200
300
400
500
600
24°N
60°E
30°N
60°E
50
100
150
150km
V.E.= 2X
A
B

FIGURE 12

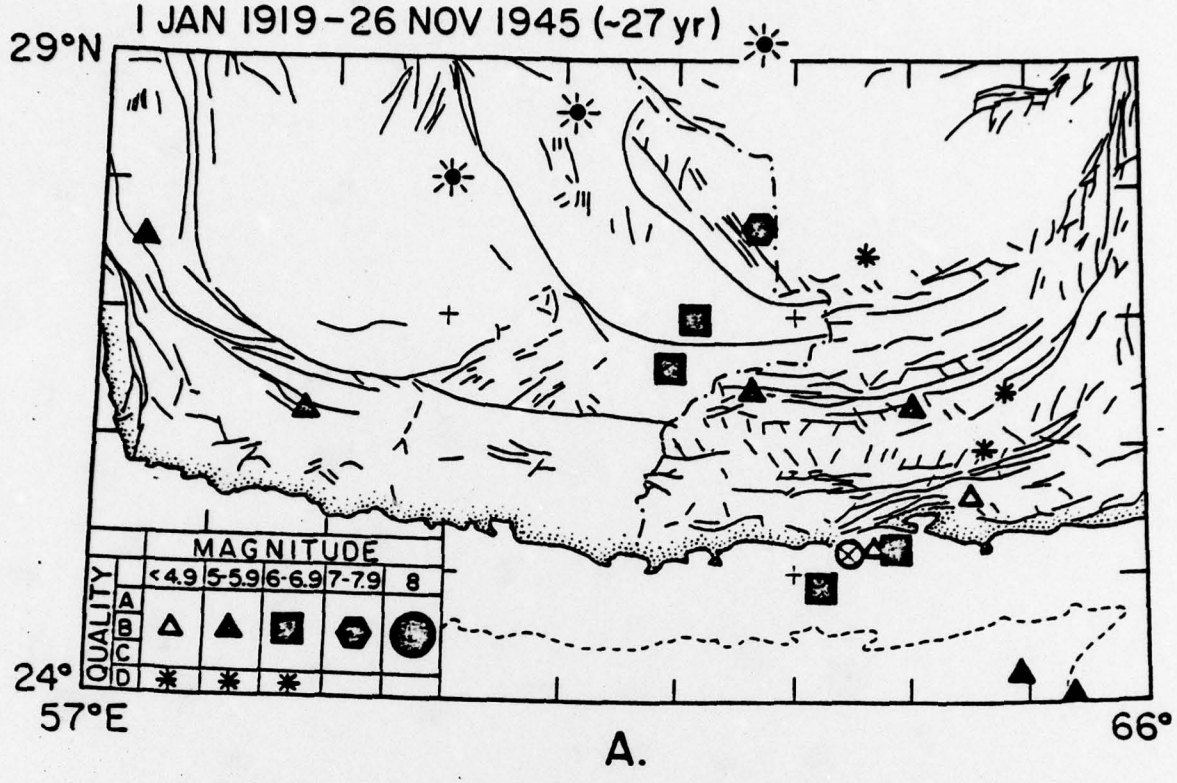
1 JAN 1919 – 26 NOV 1945 (~27 yr)
29°N
24°
57°E
66°
MAGNITUDE
QUALITY
< 4.9
5-5.9
6-6.9
7-7.9
8
A
B
C
D

A.

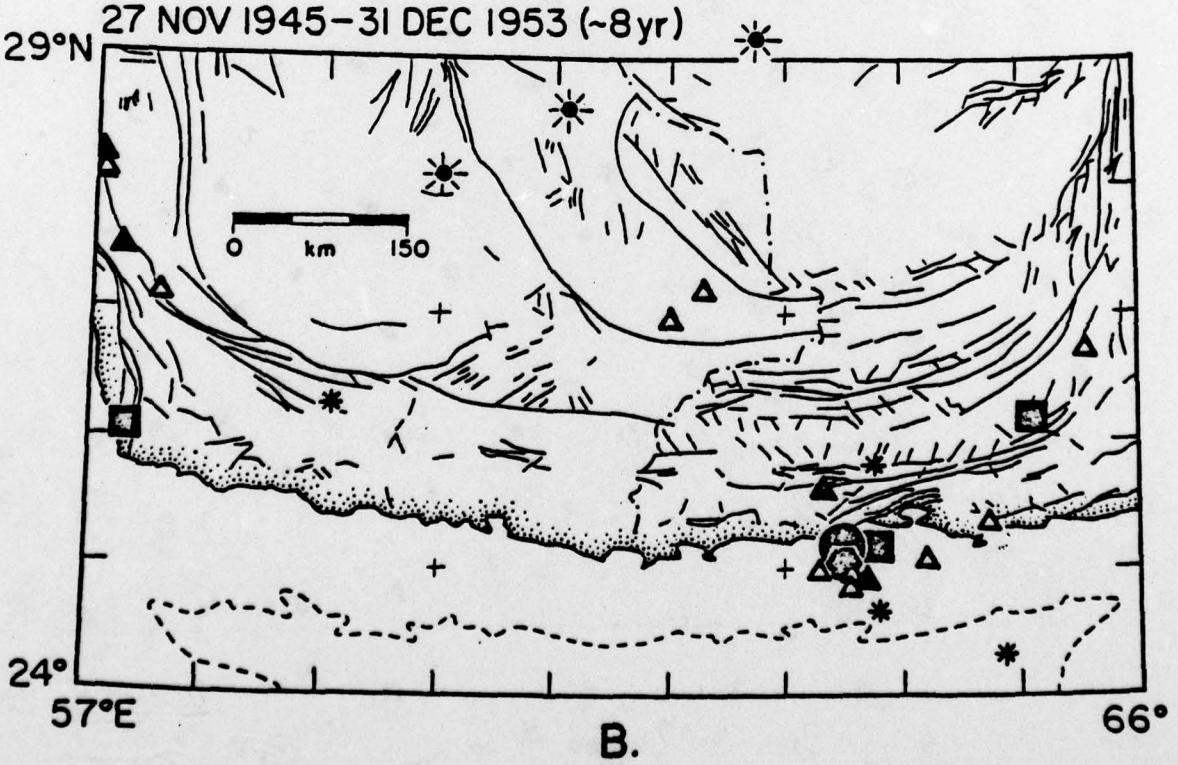
27 NOV 1945 – 31 DEC 1953 (~8 yr)
29°N
24°
57°E
66°
0
km
150

B.

FIGURE 13

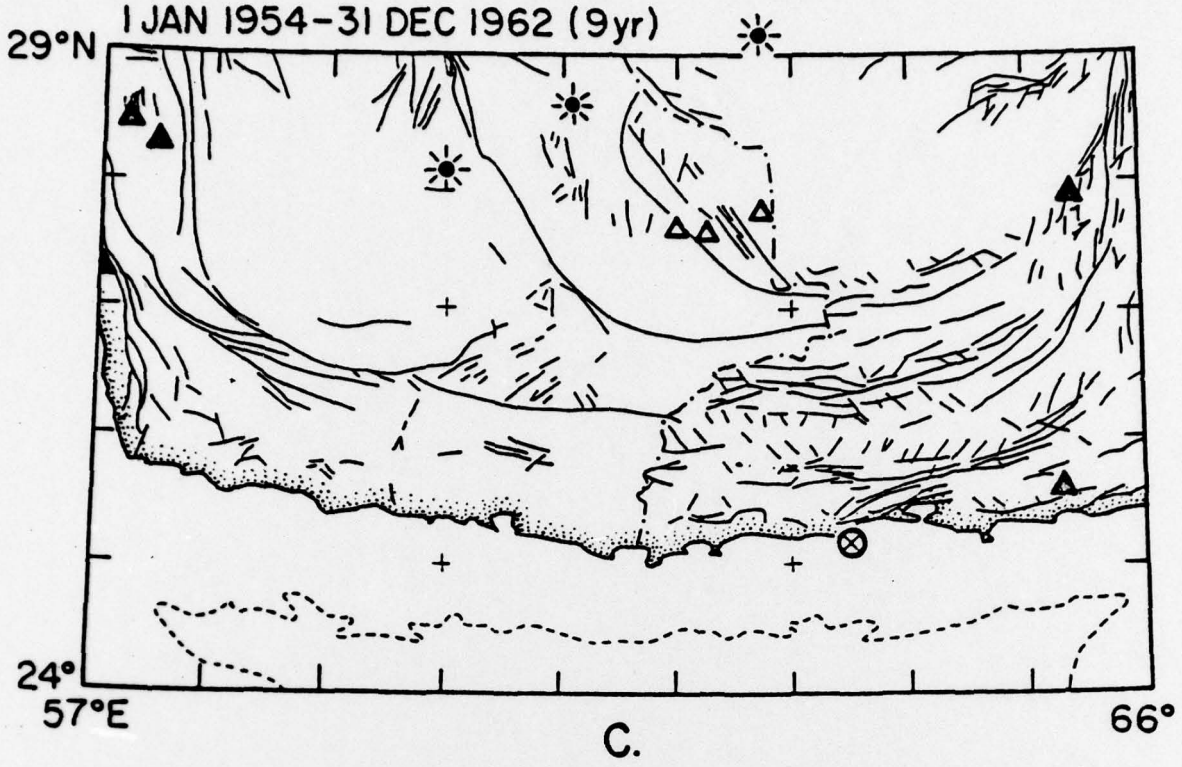
1 JAN 1954-31 DEC 1962 (9yr)
29°N
24°
57°E
66°

C.

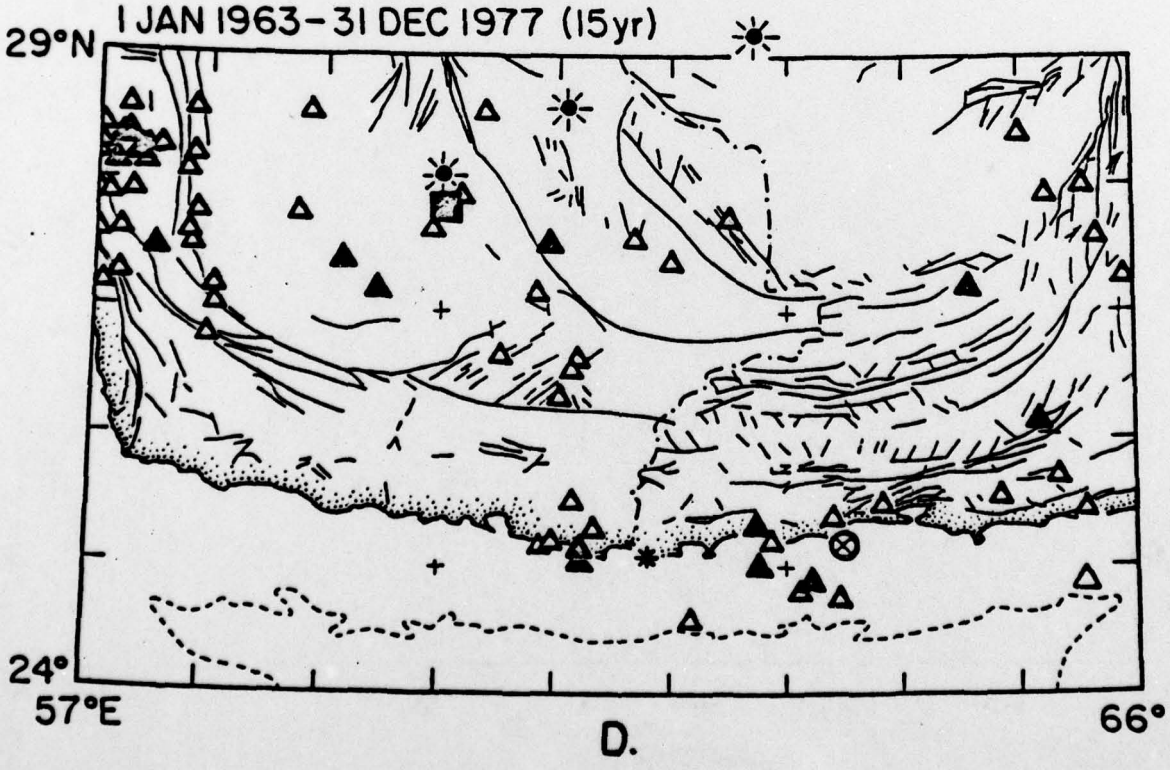
1 JAN 1963-31 DEC 1977 (15yr)
29°N
24°
57°E
66°

D.

FIGURE 13

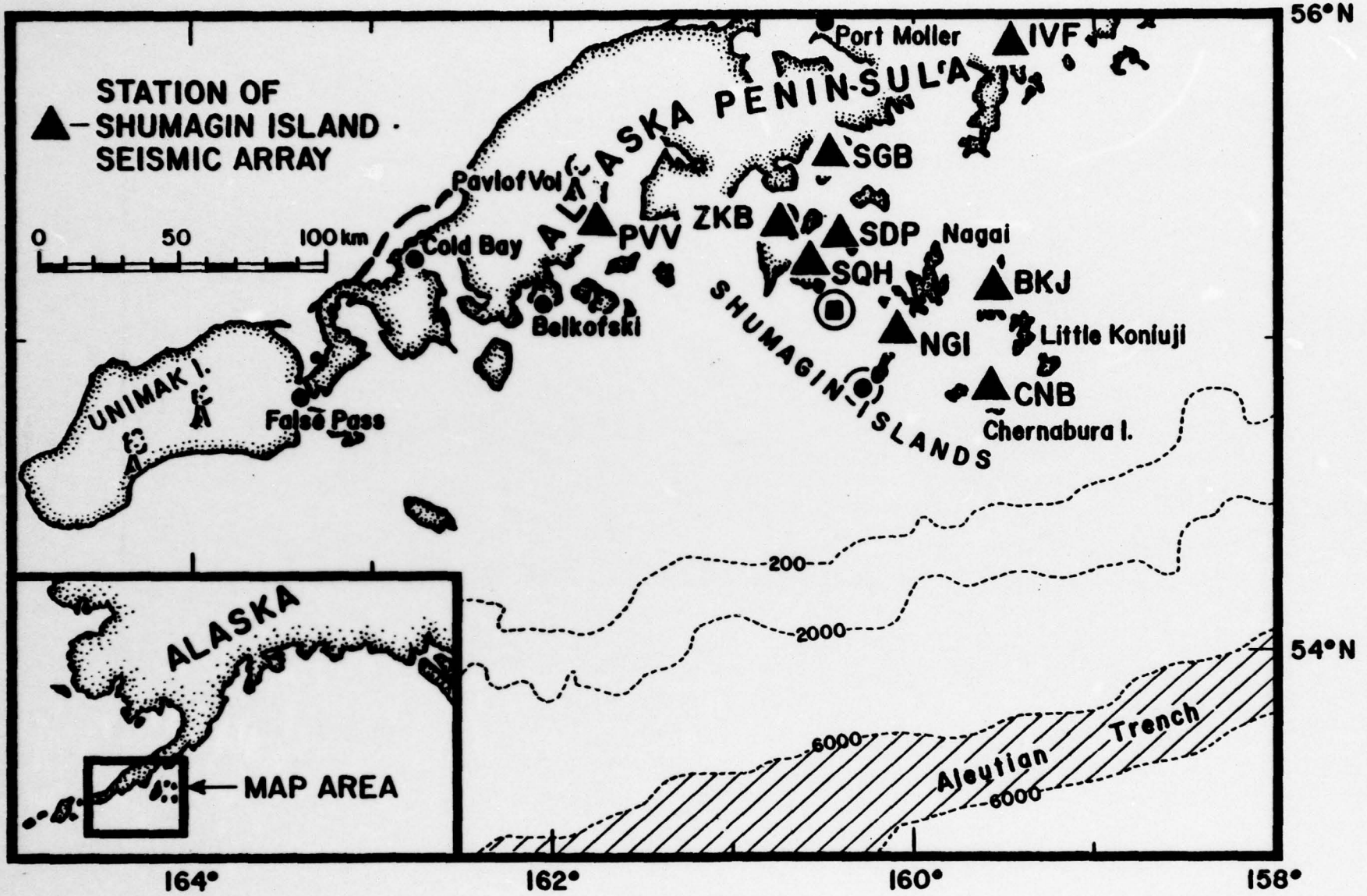

Figure 14. Location map of the Shumagin Islands and April 6, 1974 earthquakes (solid dot in circle). Shumagin network seismic stations are indicated by triangles and three letter station circles. For comparison the (mislocated) PDE epicenter is also shown (solid square in circle).

Figure 15. Cross section views of hypocenters of the main shocks and well located aftershocks. Symbol size is scaled to magnitude; full symbols are "A" quality locations; 1/2 full are "B" quality; empty are "C" quality. Tick marks are at 5 km intervals, both horizontally and vertically. Approximate rupture zone dimensions of the main shocks, as obtained from analysis of the SMA records, are dashed.

Figure 15a. Vertical cross section oriented normal to the arc. "View" is N60°E. The 0153 main shock is the shallower of the two. Note the distribution of events (especially the A and B quality) about a plane with a clip of approximately 30° northwest (left in the figure).

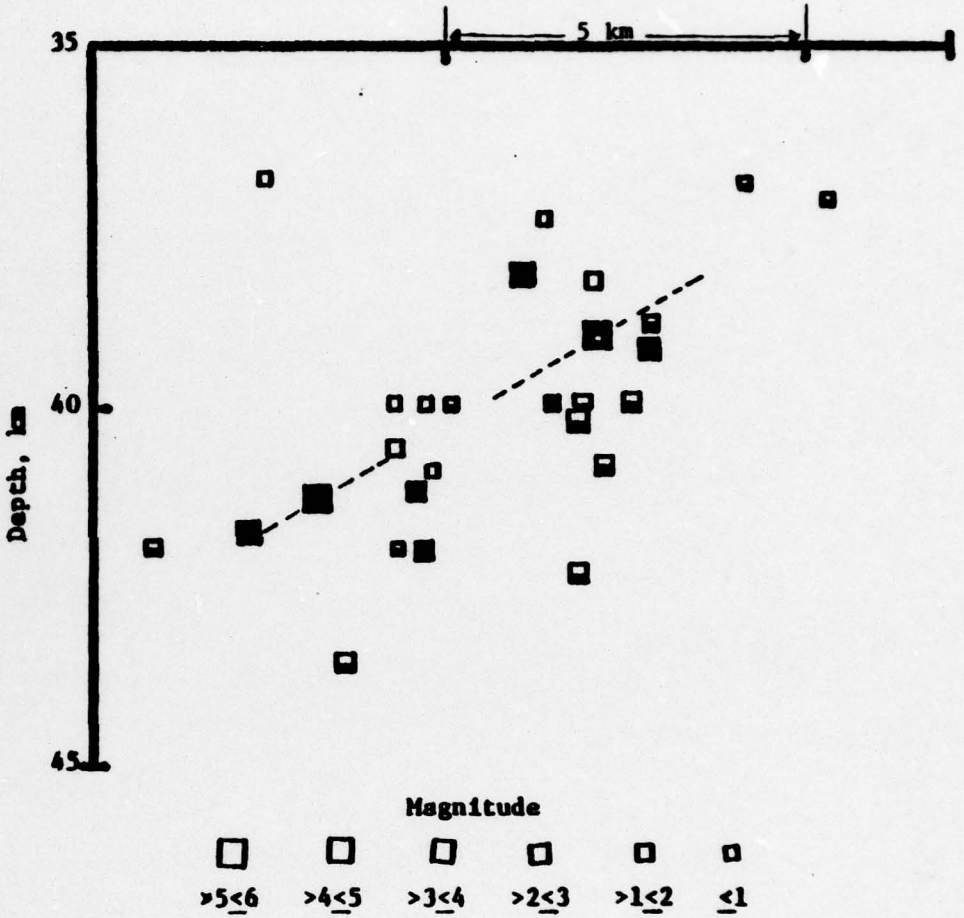

Figure 15b. Inclined cross section oriented parallel to the 30° dipping plane from (a). "View" is upward at the plane of the Benioff zone, with northeast to the right of the figure and down dip of the Benioff zone down in the figure. Note the separation of aftershocks of the two events.

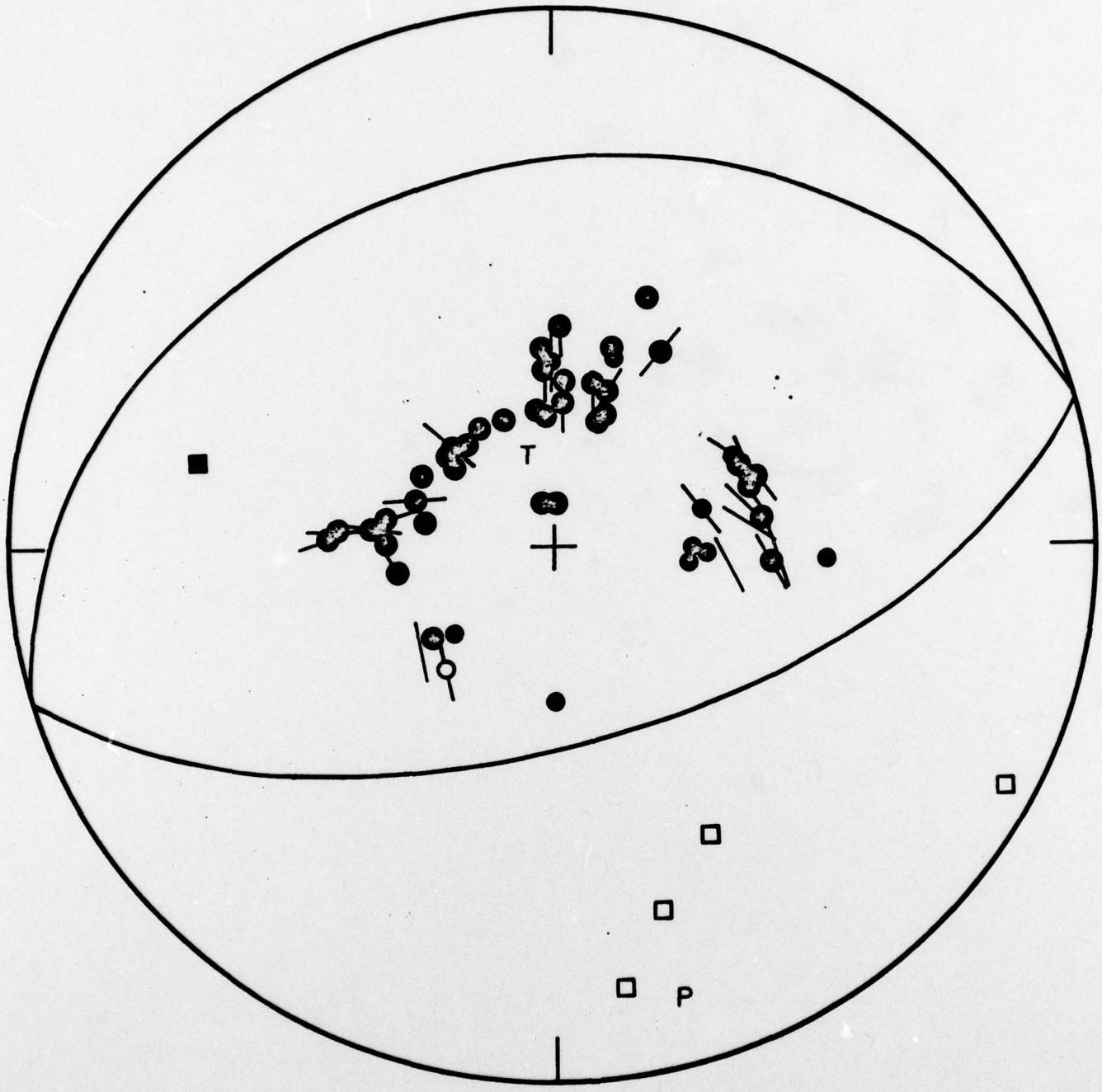

Figure 16. Focal mechanism of the 0356 hrs event on April 5, 1974. First motions and S-wave polarizations are projected onto a lower hemisphere, equal area net. WWSSN long period first motions are circles, filled are compressions, empty dilatations; smaller symbols are less reliable data. Local network short period first motions are squares; filled are compressions; empty, dilatations. S-wave polarizations are lines on figure, less reliable determinations are only half the length.

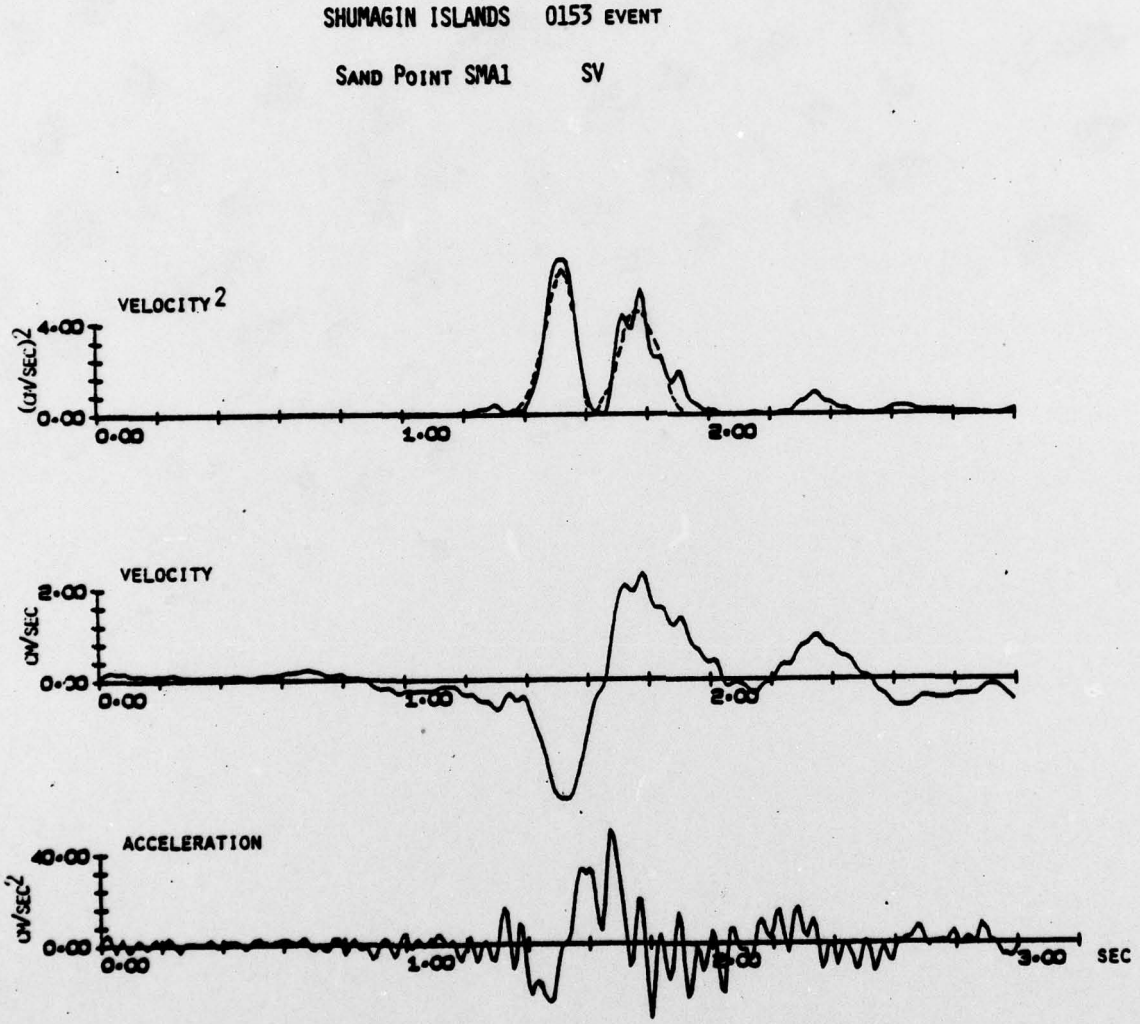

Figure 17. S_V component of S wave for 0153 event, April 6, 1974. Bottom: instrument and free surface corrected acceleration. Center: Velocity trace obtained from integrating baseline corrected acceleration. Top: Velocity-squared trace; dashed line is velocity-squared trace of final model.

SHUMAGIN ISLANDS 0356 EVENT

SAND POINT SMA1 SV

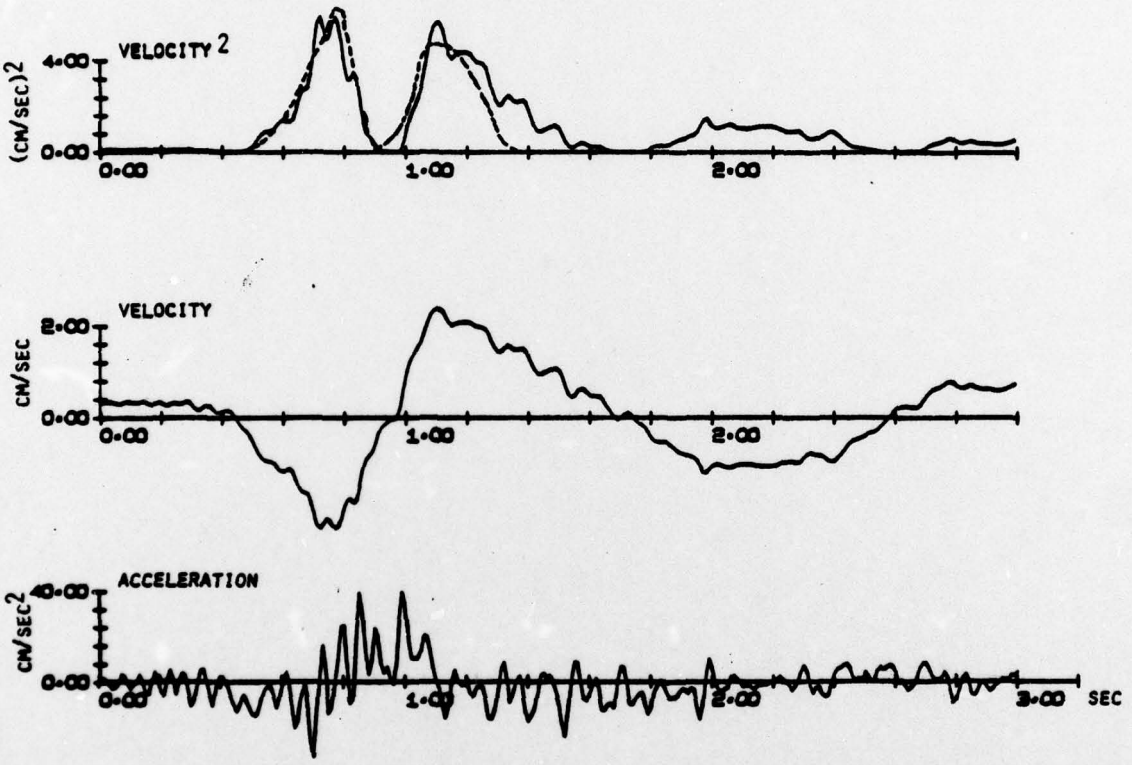

Figure 18. S_v component of S wave for 0356 event, April 6, 1974. Description similar to that of Figure 12.

REFERENCES

Alsop, L.E., A.S. Goodman, and S. Gregersen, 1974. Reflection and transmission of inhomogeneous waves with particular application to Rayleigh waves, Bull. Seism. Soc. Am., 64, 1635-1652.

Armbruster, J., L. Seeber, and K.H. Jacob, 1978. The northwestern termination of the Himalayan Mountain front: Active tectonics from microearthquakes, J. Geophys. Res., 83, 269-282.

Bhattacharya, S.N., 1971. Seismic surface-wave dispersion and crust-mantle structure of Indian Peninsula, Indian J. Met. Geophys., 22, 179-186.

Boatwright, J., 1978b. Pseudo-dynamic models of simple earthquakes and the implications of energy flux pulse shapes as modelling constraints, Abstract for XII Symposium on Mathematical Geophysics, Caracas, Venezuela.

Boatwright, J., 1979. A spectral theory for circular seismic sources; simple estimates of source dimension, *effective stress and radiated energy*, submitted to BSSA.

Brune, J., and J. Dorman, 1963. Seismic waves and earth structure in the Canadian shield, Bull. Seis. Soc. Am., 53, 167-210.

Chen, T.C., and L.E. Alsop, 1979. Reflection and transmission of obliquely incident Rayleigh waves at vertical discontinuity between two welded quarter-spaces, Submitted to BSSA.

Chen, T.C., and D.W. Forsyth, 1978. A detailed study of two earthquakes seaward of the Tonga trench: Implications for mechanical behavior of the oceanic lithosphere, Jour. Geophys. Res., 83, 4995-5004.

Chen, N.P., and P. Molnar, 1975. Short-period Rayleigh-wave dispersion across the Tibetan Plateau, Bull. Seis. Soc. Am., 65, 1051-1057.

Chun, K.Y., and T. Yoshii, 1977. Crustal structure of the Tibetan Plateau: A surface-wave study by a moving window analysis, Bull. Seism. Soc. Am., 67, 735-750.

Davies, J.N., and L. House, 1978. Aleutian subduction zone seismicity, volcano-trench separation and their relation to great thrust-type earthquakes, Accepted for publication in the Jour. Geophys. Res., JGR MS #4847.

Engdahl, E.R., and C.H. Scholz, 1977. A double Benioff zone beneath the Central Aleutians: An unbending of the lithosphere, Geophys. Res. Let., 4, 473-476.

Farhoudi, G., and D. Karig, 1977. Makran of Iran and Pakistan as an active arc system, Geology, 5, 664-668.

Fletcher, J.B., M.L. Sbar, and L.R. Sykes, 1978. Seismic trends and travel-times residuals in eastern North America and their tectonic implications, Geol. Soc. Am. Bull., 89, 1656-1676.

Forsyth, D.W., 1975. Fault plane solutions and tectonics of the South Atlantic and Scotia Sea, J. Geophys. Res., 80, 1429-1443.

Gupta, H.K., and H. Narain, 1967. Crustal structure in the Himalayan and Tibet Plateau region from surface-wave dispersion, Bull. Seis. Soc. Am., 57, 235-248.

Jacob, K.H., K. Nakamura, and J.N. Davies, 1977. Trench-volcano gap along the Alaska-Aleutian Arc: Facts and speculations in the role of terrigenous sediments for subduction, In: Island Arcs, Deep-Sea Trenches, and Back Arc Basins, (eds., M. Talwani and W. Pitman III), Maurice Ewing Series, 1, 243-258.

Jacob, K.H., and R.C. Quittmeyer, 1979. The Makran region of Pakistan and Iran: Trench-arc system with active plate subduction, In: Geodynamics of Pakistan - A Progress Report (eds. A. Farah and K. DeJong), Spec. Publ. Geol. Survey Pakistan, Quetta (in press).

Kelleher, J., and J. Savino, 1975. Distribution of seismicity before large strike slip and thrust-type earthquakes, J. Geophys. Res., 80, 260-271.

Kono, M., 1974. Gravity anomalies in east Nepal and their implications to the crustal structure of the Himalayas, Geophys. J., 39, 283-299.

Landisman, M., A. Dziewonski, and Y. Sato, 1969. Recent improvements in the analysis of surface wave observations, Geophys. J. Roy. Astron. Soc., 17, 369-403.

McGarr, A. and L.E. Alsop, 1967. Transmission and reflection of Rayleigh waves at vertical boundaries, J. Geophys. Res., 72, 2169-2180.

McKenzie, D.P., 1972. Active tectonics of the Mediterranean Region, Geophys. J. Roy. astr. Soc., 30, 109-185.

McKenzie, D.P. and J.G. Sclater, 1971. The evolution of the Indian Ocean since the late Cretaceous, Geophys. J. Roy. astr. Soc., 24, 437-528.

Minster, J.B., T.H. Jordon, P. Molnar and E. Haines, 1974. Numerical modelling of instantaneous plate tectonics, Geophys. J.R. astr. Soc., 36, 541-576.

Mogi, K., 1969. Some features of recent seismic activity in and near Japan (2), Bull. Earthq. Res. Inst., Univ. of Tokyo, 47, 395-417.

Quittmeyer, R.C., 1979. Seismicity variations in the Makran region of Pakistan and Iran: Relation to great earthquakes, in preparation.

Quittmeyer, R.C., A. Farah, and K.H. Jacob, 1979. The seismicity of Pakistan and its relation to surface faults, In: Geodynamics in Pakistan - Progress Report, (A. Farah and K. DeJong, eds.), Spec. Publ. Geol. Survey Pakistan, Quetta, in press.

Quittmeyer, R.C., and K.H. Jacob, 1979. Historical and modern seismicity of Pakistan, Afghanistan, northwestern India and southeastern Iran, Bull. Seis. Soc. Am., in press.

Saito, M., 1967. Excitation of free oscillations and surface waves by a point source in a vertically heterogeneous Earth, J. Geophys. Res., 72, 3689-3699.

Santo, T., and Y. Sato, 1966. World-wide survey of the regional characteristics of group velocity of Rayleigh waves, Bull. Earthquake Res. Inst., Tokyo Univ., 44, 939-964.

Seeber, L., and J. Armbruster, 1979. Seismicity of the Hazara Arc in northern Pakistan: Décollement vs. basement faulting, In: Geodynamics in Pakistan - A Progress Report, (A. Farah and K. DeJong, eds.), Spec. Publ. Geol. Survey Pakis-

tan, Quetta, in press.

Seeber, L., and K.H. Jacob, 1977. Microearthquakes survey of northern Pakistan: Preliminary results and tectonic implications, In: Himalaya Sciences de la terre, Éditions du Centre National de la Recherche Scientifique, No. 268, 347-360.

Solomon, S.C., 1973. Shear wave attenuation and melting beneath the Mid-Atlantic Ridge, J. Geophys. Res., 78, 6044-6059.

Sykes, L.R., 1967. Mechanism of earthquakes and nature of faulting on the mid-ocean ridges, J. Geophys. Res., 72, 2131-2153.

Sykes, L.R., 1978. Intraplate seismicity, reactivation of pre-existing zones of weakness, alkaline magmatism, and other tectonism postdating continental fragmentation, Rev. Geophys. and Spa. Phys., 16, 621-688.

Tectonic Map Compiling Group, Institute of Geology, Academia Sinica, 1974. A preliminary note on the basic tectonic features and their development in China, Scientia Geologica Sinica, 1, 1-17.

Tsai, Y.B., and K. Aki, 1970. Precise focal depth determinations from amplitude spectra of surface waves, J. Geophys. Res., 75, 5729-5743.

Weidner, D.J., and K. Aki, 1975. Focal depth and mechanism of mid-ocean ridge earthquakes, J. Geophys. Res., 78, 1818-1831.

REPORT DOCUMENTATION PAGE

READ INSTRUCTIONS BEFORE COMPLETING FORM

1. REPORT NUMBER: AFOSR-TR-79-0458	2. GOVT ACCESSION NO.
3. RECIPIENT'S CATALOG NUMBER	
4. TITLE (and Subtitle): SUTURE ZONES, SEISMIC WAVE PROPAGATION, AND TECTONICS OF CENTRAL ASIA	5. TYPE OF REPORT & PERIOD COVERED: Final Rept. 1 Oct 1976 to 30 Sept 1978
	6. PERFORMING ORG. REPORT NUMBER
7. AUTHOR(s): Thomas Chen, Richard C. Quittmeyer, Lynn R. Sykes	8. CONTRACT OR GRANT NUMBER(s): F49620-77-C-0008; ARPA Order-3291
9. PERFORMING ORGANIZATION NAME AND ADDRESS: Columbia University in the City of New York, Box 20, Low Memorial Library, New York, NY 10027 (Lamont-Doherty Geol. Obs., Palisades, NY 10964)	10. PROGRAM ELEMENT, PROJECT, TASK AREA & WORK UNIT NUMBERS: 62701E 8F10 3291-19
11. CONTROLLING OFFICE NAME AND ADDRESS: Advanced Research Projects Agency/NMR, 1400 Wilson Blvd., Arlington, VA 22209	12. REPORT DATE: Sept 1978
	13. NUMBER OF PAGES: 54
14. MONITORING AGENCY NAME & ADDRESS (if different from Controlling Office): Air Force Office of Scientific Research/NP, Bldg. 410, Bolling AFB, DC 20332 (12) 55 p.	15. SECURITY CLASS. (of this report): Unclassified
	15a. DECLASSIFICATION/DOWNGRADING SCHEDULE

16. DISTRIBUTION STATEMENT (of this Report)

Approved for public release; distribution unlimited.

17. DISTRIBUTION STATEMENT (of the abstract entered in Block 20, if different from Report)

18. SUPPLEMENTARY NOTES

19. KEY WORDS (Continue on reverse side if necessary and identify by block number)

Reflection/transmission coefficients, numerical methods, group velocities, Rayleigh waves, Love waves, surface waves, crustal velocities, Tibet, P-wave residuals, suture zones, New York State, Vermont, Quebec, focal mechanism, Mid-Atlantic ridge, Algeria, magnitude-yield relation, intraplate seismicity, Central Asia, Pakistan, composite fault-plane solutions, microseismicity, Himalayas,

20. ABSTRACT (Continue on reverse side if necessary and identify by block number)

The results of a number of projects are summarized:

1. An approximate method for calculating the reflection and transmission coefficients of obliquely incident Rayleigh waves across two welded quarter-spaces is outlined.

2. Group velocities of fundamental mode Rayleigh and Love waves, with paths traversing the Tibetan Plateau, were used to determine that the

next page

DD FORM 1 JAN 73 1473 EDITION OF 1 NOV 65 IS OBSOLETE

UNCLASSIFIED

SECURITY CLASSIFICATION OF THIS PAGE (When Data Entered)

Block 19 (con't.):

Hazara arc, historical seismicity, Makran, subduction, volcanism, Benioff zone, seismic gaps, Aleutians, stress-drop, strong-motion accelerograms, lithosphere, aftershocks.

Block 20 (con't.):

Tibetan Plateau has a 70 km thick crust, with a low velocity zone at an intermediate level within the crust.

3. A zone of large, negative residuals for P-wave arrivals exists in northern New York State.

4. Surface-wave amplitude spectra constrained by body-wave first motions are sufficient to determine focal mechanisms for some moderate-sized earthquakes along the Mid-Atlantic ridge.

5. The French test site in Algeria has, contrary to previous belief, not been tectonically stable since the Precambrian. Thus, seismic waves leaving this region may be more attenuated than was previously suspected. Yield estimations for the French test site will have to be re-evaluated.

6. Microseismicity and geological evidences were used to model the current tectonic processes of the Hazara district in northern Pakistan.

7. The historical and modern seismicity of a portion of south-central Asia was compiled and critically reviewed to delineate large-scale seismotectonic trends.

8. Seismic, volcanic, and plate tectonic data indicate the Makran region of southern Pakistan is an active subduction zone.

9. Seismicity and tectonics of the Aleutians, Alaska were studied. Large stress-drops (∿ 500 bars) for two earthquakes were determined from strong-motion accelerograph records.

10. A focal mechanism study and aftershocks survey were undertaken for a large intraplate earthquake 350 km southwest of Bermuda.

11. A comparative surface-wave technique was used to precisely determine the depths of two earthquakes that occurred seaward of the Tonga trench. Implied stresses for these earthquakes are consistent with bending of an elastic plate model.